The Effect of Pseudo-Global Warming on the Weather-Climate System of Africa in a Convection-Permitting Model

Kelly M Nunez Ocasio[1] and Erin Dougherty[2]

[1]NCAR
[2]National Center for Atmospheric Reserach

March 15, 2024

Abstract

The weather-climate system of Africa encompassing the African easterly jet (AEJ) and the West African Monsoon (WAM) can largely modulate high-impact weather over Africa and the tropical Atlantic. How the weather-climate system of Africa will change with a warming climate is just starting to be addressed due to global climate model limitations in resolving convection. We employ a novel atmospheric convection-permitting model regional setup alongside the pseudo-global warming (PGW) approach to address climate change impacts on the weather-climate system of Africa. Our findings indicate that the AEJ and areas of monsoon flow intensify in a future warming climate scenario together with an increase in monsoonal moisture. Moreover, precipitation will increase over high topography and shift southward due to a latitudinal expansion and increase of deep convection closer to the equator. This has relevant ramifications for the livelihood of communities that depend on water-fed crops in tropical Africa.

The Effect of Pseudo-Global Warming on the Weather-Climate System of Africa in a Convection-Permitting Model

K. M. Núñez Ocasio[1], Erin M. Dougherty[1]

[1]NSF National Center for Atmospheric Research, Boulder, CO, USA

Key Points:

- The weather-climate system of Africa is explored with the novel use of a convection-permitting model and the pseudo-global warming method.
- The African easterly jet and areas of monsoon flow will intensify in a warming climate scenario together with increased monsoon moisture.
- An increase in precipitation is expected in a future warming climate scenario over the monsoon, high topography, and the eastern Atlantic.

Corresponding author: Kelly M. Núñez Ocasio, knocasio@ucar.edu

Abstract

The weather-climate system of Africa encompassing the African easterly jet (AEJ) and the West African Monsoon (WAM) can largely modulate high-impact weather over Africa and the tropical Atlantic. How the weather-climate system of Africa will change with a warming climate is just starting to be addressed due to global climate model limitations in resolving convection. We employ a novel atmospheric convection-permitting model regional setup alongside the pseudo-global warming (PGW) approach to address climate change impacts on the weather-climate system of Africa. Our findings indicate that the AEJ and areas of monsoon flow intensify in a future warming climate scenario together with an increase in monsoonal moisture. Moreover, precipitation will increase over high topography and shift southward due to a latitudinal expansion and increase of deep convection closer to the equator. This has relevant ramifications for the livelihood of communities that depend on water-fed crops in tropical Africa.

Plain Language Summary

The weather-climate system of Africa is closely linked to high-impact weather events, such as storms and African easterly waves, which can lead to tropical cyclones. Studying how the weather-climate system of Africa will change with a warming climate is a recent research focus. In our study, we use a novel weather model to investigate these changes. By adjusting the model to reflect a future warming climate scenario, we discover that the African easterly jet, convection, and West African Monsoon will become stronger. Additionally, rainfall will increase in the monsoonal region and shift southward. This information is vital, as it significantly affects communities relying on water-fed crops.

1 Introduction

The weather-climate system of Africa comprises of the African easterly jet (AEJ) sustaining African easterly waves (AEWs), the West African Monsoon (WAM), and associate convection. The AEJ arises from thermal wind balance over the northern summer months due to the very warm and dry Saharan desert over North Africa and the relatively cooler and moist conditions south of it (Pytharoulis & Thorncroft, 1999). The interactions between the AEJ and the WAM can dictate monsoonal precipitation patterns (Diallo et al., 2013; Sylla et al., 2013; Pytharoulis & Thorncroft, 1999; Hsieh & Cook, 2007; Bercos-Hickey et al., 2020), and the formation, growth, and propagation of mesoscale convective systems (MCSs) and AEWs which can serve as tropical cyclone (TC) precursors (Landsea, 1993; Núñez Ocasio et al., 2021, 2020b; Rajasree et al., 2023). Both AEWs and MCSs are high-impact weather events embedded within the complex African weather-climate system.

Few studies have specifically addressed how the AEJ-AEW system and WAM may change in a warming climate (Skinner & Diffenbaugh, 2014; Hannah & Aiyyer, 2017; Brannan & Martin, 2019; Kebe et al., 2020; Bercos-Hickey & Patricola, 2021; Bercos-Hickey et al., 2023). This is largely due to global climate models (GCMs) and regional models with deep convection parameterized not properly resolving the complex moisture-convective feedbacks and the multi-spatial nature of the weather-climate system of Africa (Cornforth et al., 2009; Janiga & Thorncroft, 2013; Tomassini et al., 2017; Núñez Ocasio et al., 2020a; Núñez Ocasio & Rios-Berrios, 2023).

For example, Kebe et al. (2020) found a future intensification and southern shift of the AEJ related to a shift in the meridional temperature gradient causing a decrease in AEW activity. Skinner and Diffenbaugh (2014) found an intensification of the meridional temperature gradient and the AEJ although they did not establish a consistent movement of the location of the jet. They also found an increase in low-level westerly flow beneath the jet and in AEW activity. Using a regional WRF configuration with a relatively coarse resolution of 27 km and parameterized convection, Bercos-Hickey and Patricola (2021) found that the AEJ weakens, shifts poleward, and is located at a higher altitude in the future climate with increased precipitation and low-level westerlies over the Sahel region. They also show an increase in the strength of the meridional temperature gradient. These results are similar to Núñez Ocasio et al. (2024) moisture sensitivity experiments except that they show that the AEJ is more intense in a moister environment. Noteworthy is that Núñez Ocasio et al. (2024) study uses a novel convection-permitting regional setup using the Model for Prediction Across Scales-Atmosphere (MPAS-A). Although moisture-sensitivity experiments like these cannot be directly related to climate projection experiments for which the role of temperature and anthropogenic sources are considered, the comparison can help elucidate the role of moist-convective processes in the weather-climate system of Africa and their connection to AEWs. These few studies present conflicting findings regarding the future trajectory of the AEJ, the meridional temperature gradient over North Africa, and, consequently, precipitation patterns, as well as the intensity and frequency of AEWs.

To capture the effect of thermodynamic changes due to anthropogenic-induced warming, this study applies a pseudo-global warming (PGW) method over a several day period of high-impact weather in Africa in convection-permitting simulations. The PGW method adds a perturbation representative of a future climate state to renanalysis data to understand how today's weather will change under warmer and moister conditions (Schär et al., 1996). While the PGW method has been applied in the mid-latitudes to study regional climate change impacts at convection-permitting scales on convection (Prein et al., 2017; Rasmussen et al., 2020; Dougherty et al., 2023), heavy rainfall (Schär et al., 1996; Kawase et al., 2009; Lackmann, 2013; Ban et al., 2015; Dougherty & Rasmussen, 2020), and atmospheric rivers (Mahoney et al., 2013; Dougherty et al., 2020), very few studies have utilized this approach to study climate change impacts on tropical precipitation, aside from Heim et al. (2023) and Bercos-Hickey and Patricola (2021). However, even studies that have applied the PGW method to the tropics use the WRF model, whereas this is the first study to apply it to the MPAS-A model.

Understanding how the weather-climate system of Africa evolves with climate change using convection-permitting modeling can enhance our ability to assess the critical implications of environments conducive to high-impact weather such as tropical cyclones and AEWs. This is the first study to the authors' knowledge that applies the PGW method to a Model for Prediction Across Scales-Atmosphere (MPAS-A) regional variable-resolution configuration introduced in Núñez Ocasio et al. (2024) that is capable of simulating processes at convection-permitting scales.

This study aims to answer the following scientific question:

Q: What are the short-term changes to the African weather-climate system in a future warmer climate scenario?

2 Methods and Data

2.1 MPAS Configuration

The Model for Prediction Across Scales-Atmosphere (MPAS-A) version 8.0.1 with the Limited-Area configuration was used for this study (Skamarock et al., 2012; Núñez Ocasio & Dougherty, 2024) to simulate the period of 1200 UTC 8 September–1800 UTC 13 September 2006 as in Núñez Ocasio and Rios-Berrios (2023); Núñez Ocasio et al. (2024).

Various features were active during this period including AEWs, MCSs, WAM, and ITCZ, all while during field campaigns NAMMA and AMMA (Zipser et al., 2009). In addition to initializing the model at 1200 UTC on 8 September, two other sets of experiments were completed: initializing the model at 00 UTC on 5 September and initializing at 00 UTC on 6 September. In incorporating three sets of experiments, we can account for spinup and the sensitivity to small perturbations for precipitation details given the short integration period.

The Limited-Area domain is from 30°S to 51°N and 65°W to 59°E depicted in Núñez Ocasio and Dougherty (2024)(and in Núñez Ocasio et al. (2024) their Figure 1). A 15-km–3-km variable-resolution mesh was used with the 3-km high-resolution refinement region elliptically shaped. The mesh was rotated over North Africa and the eastern Atlantic to ensure the track of AEWs and the inclusion of the ITCZ, AEJ, and WAM within the refined region.

The "convection permitting" physics suite was used here as in Núñez Ocasio et al. (2024). The scale-aware Grell-Freitas convection parameterization scheme (Grell & Freitas, 2014) changes from parameterized deep convection at the hydrostatic scales (parameterized grid is at 15 km) to only parameterize shallow convection in the refined 3-km region. At 3 km, deep convection was explicitly resolved. The rest of the schemes include RRTMG shortwave and longwave radiation (Iacono et al., 2008), Xu-Randall subgrid cloud fraction (Xu & Randall, 1996), MYNN boundary-layer and surface-layer schemes (Nakanishi & Niino, 2004), Noah land-surface scheme (Niu et al., 2011), and Thompson microphysics (Thompson et al., 2008).

The model was configured to run with 55 levels. Model outputs in the native unstructured grid were hourly. Native model output was vertically interpolated to obtain isobaric variables with 27 isolevels. The model output was spatially interpolated to a latitude and longitude grid equivalent of a 0.25°×0.25° horizontal resolution. The interpolation used a first-order conservative Gaussian grid (Jones, 1999) as done in Núñez Ocasio and Rios-Berrios (2022); Núñez Ocasio (2023).

2.2 Pseudo-global Warming Experiment

The ECMWF reanalysis 5th Generation (ERA5; Hersbach et al., 2020) was used to initiate the model and provide lateral boundary conditions hourly for the control (CTRL) simulations. The PGW experiments are the same as the CTRL experiments, except a delta signal representative of a future climate state is added to the ERA5 forcing data at the lateral boundaries:

$$CTRL = ERA5 \tag{1}$$

$$PGW = ERA5 + \Delta LENS2 \tag{2}$$

where Δ is given by the following:

$$\Delta = (2070 - 2100)–(1991 - 2021) \tag{3}$$

The PGW experiment takes the 100-member ensemble mean difference of the Community Earth System Model (CESM) Large Ensemble (LENS) version 2 (LENS2; Rodgers et al., 2021) at the end-of-century (2070-2100) under the SSP3-7.0 future radiative forcing scenario from the historical period (1991-2021). The perturbed variables from LENS2 added to ERA5 include temperature, geopotential height, horizontal winds, relative humidity, sea surface temperature, soil temperature, and pressure. Perturbing pressure, geopotential height, and winds, alongside temperature and humidity, ensure balance is maintained in the atmosphere (Brogli et al., 2023). This method thus simulates similar weather patterns as the current day but under warmer and moister conditions. Using the ensemble mean from LENS2 also assures that this response is a robust climate change signal, and not due to the internal variability of the model (Huang et al., 2020).

A limitation of the study is that it uses only one future projection scenario and one climate model for simulations of short integration time. Nonetheless, the main differences between the CTRL and PGW simulations in three experiments with different initializations are noteworthy and consistent across experiments, providing confidence that our results are not just artifacts of spin-up time. The variability across the three experiments initialized at different times is also noted in the study. This demonstrates that this kind of framework can be applied to multiple future climate scenarios and longer simulations. The objective of this study is on how future climate projections will affect the weather-climate system of Africa at short time scales, and thus, the focus is on a short period.

3 Results

To validate our regional convection-permitting PGW approach, we first assess the effects of the future warming on convection and precipitation associated with the ITCZ over the eastern Atlantic and the WAM over land. The differences across CTRL and PGW simulations (Figure 1g, Figure S1g, and Figure S2g) shows higher precipitation rates in the future climate. Specifically, precipitation rates are greater in the PGW scenario over the eastern Atlantic offshore waters (part of the ITCZ and West African offshore rainfall maximum), the Guinea Highlands, Cameroon Mountains, and the offshore waters of the Bight of Benin following the coast of Nigeria, Cameroon, Equatorial Guinea, and Gabon.

Although there is a slight increase in precipitation over the Sahel in the future climate agreeing with Bercos-Hickey and Patricola (2021) findings, the more prominent increases in precipitation here are located south of 10°N. Moisture-sensitivity experiments by Núñez Ocasio et al. (2024) also show these distinct peaks in precipitation over the region of the west African coast rainfall maximum, Guinea Highlands, and over the coast of the Bight of Benin with maxima over the Cameroon Mountains. The similarities across the PGW experiment here and moist-sensitivity experiments in Núñez Ocasio et al. (2024) may suggest a key role of water vapor in modulating future precipitation extreme patterns over the ITCZ and African monsoonal belt over tropical Africa.

With respect to the WAM, it is evident from Figure 1 (second column and in S1 and S2 for the additional experiments) that monsoonal moisture will increase in the future climate scenario both over land and water consistent with the increase in precipitation. There is variability across experiments on the location and intensity of the WAM confluent zone over the continent (Figure 1i, S1i, and S2i). However, the southwesterly monsoonal flow over the Gulf of Guinea and the embedded Bight of Benin consistently shows a strengthening across all experiments in the future climate. Over the western coast of Africa a prominent cyclonic feature also exhibits intensification in the future. This feature can be a signal of both intensifying AEWs and ITCZ.

Figure 2 (as well as S3 and S4) shows a time-average latitude analysis over a longitudinal average defined as the WAM box from 15°W to 25°E. More precipitable water content across the monsoonal region is to be expected in the future climate due to moisture increases following the Clausius-Clapeyron relationship and consistent with the

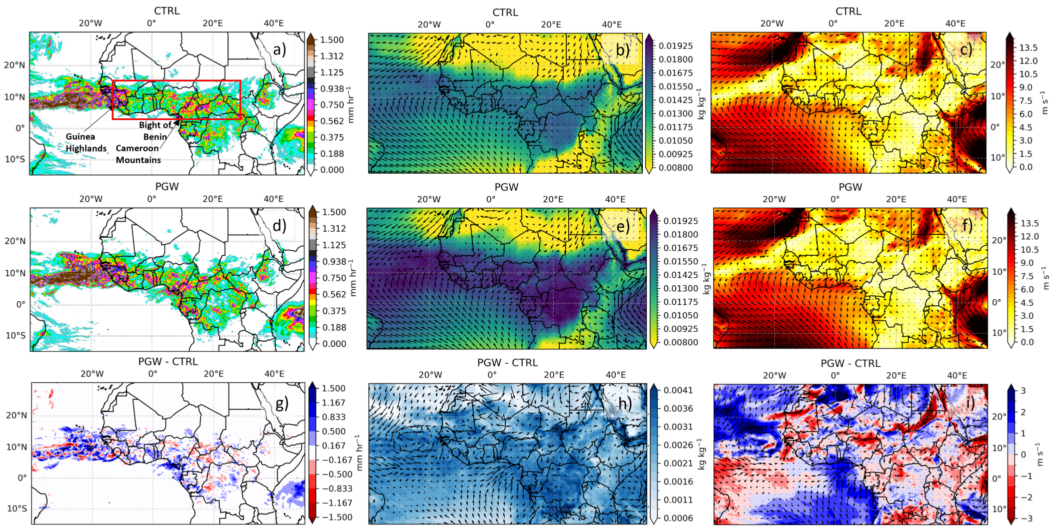

Figure 1. Time-averaged precipitation rates, 950-hPa water vapor mixing ratio (shade), and 950-hPA total winds (vectors and shade) removing the first 24 hours of the simulation for CTRL in (a), (b), and (c), respectively. The same from (d-f) for PGW and from (g-i) for the differences. Labels for Guinea Highlands, Bight of Benin, and the Cameroon Mountains are included in (a) for reference. The red square denotes the region that will be named WAM box hereon from 15°W to 25°E and 4°N to 15°N.

increase in monsoonal moisture (Figure 2; precipitable water). However, the average precipitation rate over the domain increases at less than the Clausius-Clapeyron rate of 7 % K^{-1}, with an increase of 4.8 % K^{-1}. This rate of increase is possible because we consider all precipitation, not just precipitation extremes or convection specifically, where precipitation rates are expected to increase at or above the Clausius-Clapeyron rate (Prein et al., 2017; Loriaux et al., 2013).

Convection is also deeper between 5°S and 7.5°N (Figure 2; OLR) in the future climate. Related to the deeper ITCZ and monsoonal convection in the PGW scenario, regions of peak precipitation rates are to expected to have even higher rates and the peaks will be shifted equatorward (Figure 2; precipitation rates) as was evident from Figure 1. Heim et al. (2023) similarly saw a southward shift in the precipitation maximum near the equator and intensification of the ITCZ.

Cross sections of time-average diabatic heating rates show where the maximum of moist convection for each simulation is located (Figure 3, and S5). The majority of the

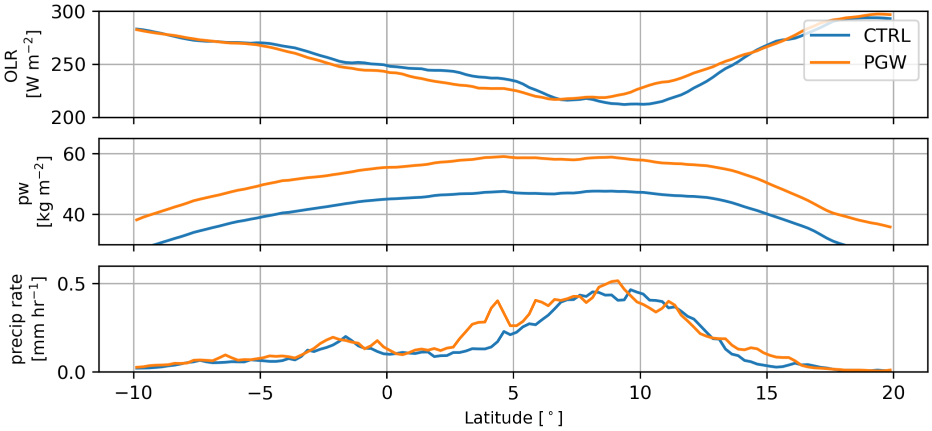

Figure 2. Latitude analyses of time-averaged, zonally averaged (top) OLR, (middle) precipitable water (pw), and (bottom) precipitation rate removing the first 24 hours of the simulation for CTRL (blue lines) and PGW (orange lines). Longitude average is taken for the WAM box.

monsoonal moist convection is located between 5°N and 15°N in the CTRL scenario with maximum between 10°N and 12°N. The future scenario exhibits a latitudinal expansion of the convection with deeper (top-heavy signature reaching above 250 hPa). Although there is variability across experiments as to where the maximum of diabatic heating difference lies (compare maxima locations in Figure 3c, S5c, and S5f) there is consistency across experimenters that deeper and more intense convection shifts to the south of 10°N in the PGW simulations. This diabatic heating signature agrees with the expected southward shift of the ITCZ and monsoonal precipitation shown in the previous figures.

Such a deepening of diabatic heating is expected in a warmer climate in the tropics, fitting with the fixed anvil temperature (FAT) hypothesis (Hartmann & Larson, 2002), whereby anvils rise in a warmer climate and thereby remain at the same temperature. Interestingly, the widening of diabatic heating contrasts the idea of a "deep-tropics squeeze" (Lau & Kim, 2015) that suggests a narrowing of the ITCZ. Similar to this idea is the "warming-induced contraction of tropical convection" hypothesis by a GCM climate change study over the tropics (Zhang, 2023), though the PGW convection-permitting simulations from Heim et al. (2023) also do not find such a pronounced narrowing of the ITCZ.

Within the weather-climate system of Africa is the AEJ which serves as an energy source for both AEWs and MCSs and plays a major role in dictating the high-impact weather over the region. Previous climatology studies have shown that the AEJ is weaker

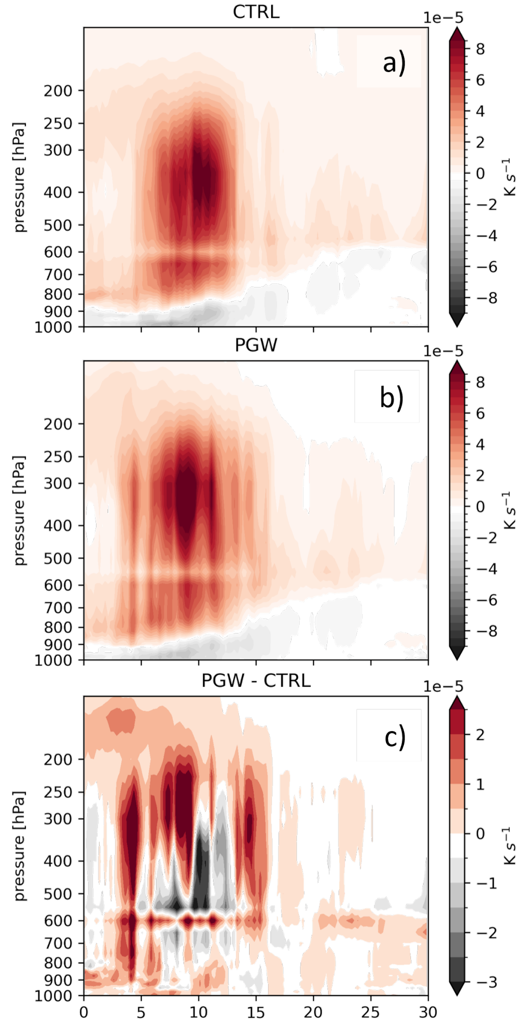

Figure 3. Vertical cross-section of the time-averaged diabatic heating rates from microphysics scheme removing the first 24 hours of the simulation for (a) CTRL, (b) PGW, and (c) the difference. Longitude average taken for WAM box. Y axis is in log scale.

and farther north during wet years (Newell & Kidson, 1984; Sylla et al., 2013; Diallo et al., 2013; Bercos-Hickey et al., 2020). In Bercos-Hickey and Patricola (2021) they found a weaker, more northward-positioned AEJ located at a higher altitude in the future climate. Similarly, the difference between PGW and CTRL here in Figure 4c (as well as in S6e and S7e) show an AEJ shifted northward in the future climate with core greater than 13 m s^{-1} located at or slightly above 15°N at 600 hPa. However, unlike Bercos-Hickey and Patricola (2021), the core of the AEJ here is more intense in the future scenario than the CTRL experiment. A stronger more northward AEJ and wetter conditions were also found in Núñez Ocasio et al. (2024) moisture-sensitivity experiments al-luding again to the role of water vapor on high-impact weather events. With the AEJ strengthening and being positioned more northward relative to the WAM confluent zone over the continent in the future climate, is less likely for the AEJ to interact with the southwesterly monsoonal flow sufficiently. This is turn inhibits significant shear production and limits the likelihood of barotropic and baroclinic energy exchanges ultimately, affecting the intensity of AEWs and the AEJ-AEW system (i.e., Núñez Ocasio et al., 2024). How the AEJ-AEW system, as well as how the intensity and frequency of AEWs and MCSs will be affected in the changing climate is out scope of this study. However, it is currently being explored and is the topic of a follow-up study.

At the larger scales, the upper-level jets such as the tropical easterly jet (TEJ) with a maximum of around 250 hPa will strengthen while the subtropical jet with the core at about 200 hPa, will weaken in the future climate scenario. The strengthening of the AEJ in the future climate scenario is related to the low-level meridional potential temperature gradient. Additionally, the stronger TEJ is consistent with a strengthening of jet stream wind projected by GCMs globally, due to an increase in the meridional humidity gradient under climate change that impacts the thermal wind via density gradients (Shaw & Miyawaki, 2023).

Within the weather-climate system of Africa, the meridional temperature gradient during the northern summer months gives rise to the AEJ through thermal wind balance. Skinner and Diffenbaugh (2014) and Bercos-Hickey and Patricola (2021) found an increase in the strength of the meridional temperature gradient. Agreeing with these studies, it is evident that in the future climate scenario here, the strength of the meridional potential temperature gradient increases across the atmospheric column (Figure 4f, S6f, and S7f). This stronger meridional potential temperature gradient relates to an increase in precipitation and monsoon intensity. The stronger meridional potential temperature gradient at the surface directly relates to the meridional potential vorticity (PV) reversal at the mid-levels that exists over the African continent during the northern summer months and satisfies the Charney-Stern criterion for dynamical instability (Pytharoulis & Thorncroft, 1999). This PV meridional gradient is also strengthened in the PGW scenario (not shown). Finally, given the evident increase in precipitation over high topography shown here in the future climate, it is noteworthy that topography like the Cameroon Mountains and the Guinea Highlands can influence the low-level meridional potential temperature gradient over Africa. This, in turn, can affect precipitation as we see here and AEW energetics (i.e., Hamilton et al., 2020, 2017).

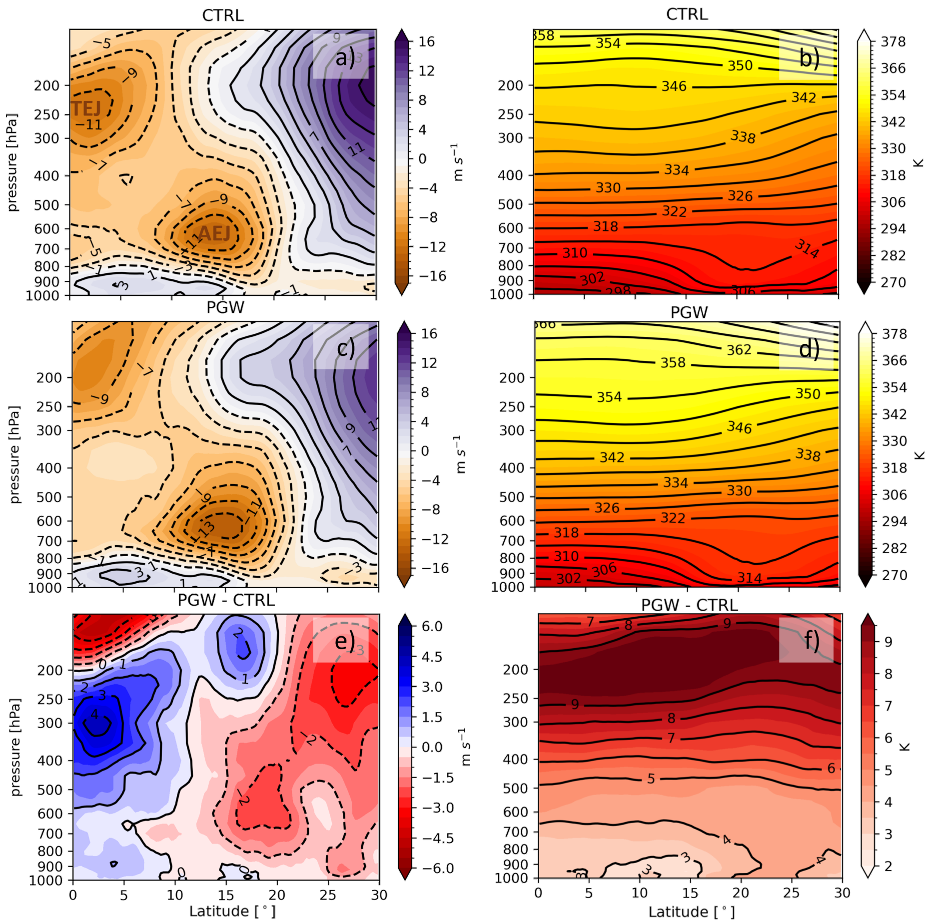

Figure 4. Vertical cross-section of the time-averaged zonal wind and potential temperature removing the first 24 hours of the simulation for CTRL in (a) and (b), respectively. The same from (c-d) for PGW, and from (e-f) for the differences. Longitude average taken for the WAM box. Y axis is in log scale. The AEJ and TEJ are labeled in (a).

4 Conclusions

Through a novel convection-permitting framework that applies the PGW method, we have addressed the question of what are the short-term changes to the weather-climate system of Africa in a future warming climate scenario.Using a convection-permitting model alongside the PGW method, we can better asses climate changes in a more realistic model setup to be able to compare our results to past studies that used GCMs and/or parameterized convection.

Although some variability is evident across the three experiments initialized at different times while using the same future climate scenario, consistent patterns emerge of how the weather-climate system of Africa will change with the changing climate. Different from past studies we find that the AEJ intensifies and shifts poleward in the future climate scenario. The ITCZ over the eastern Atlantic will intensify in a future climate scenario. An increase in precipitation rates related to a monsoonal increase in moisture is also to be expected in the future climate, especially south of 10°N. This southern shift of the precipitation is consistent with deeper and more intense convection shifting to the south of 10°N. In the future climate scenario, the southwesterly monsoonal flow over the Gulf of Guinea and the embedded Bight of Benin intensifies. Agreeing with past studies, we show an increase in the strength of the meridional temperature gradient. This strengthening is related to the intensification of both the AEJ at the mid-levels and of the TEJ.

The AEJ serves as an energy source for AEWs, and the WAM and ITCZ provide a moisture-favorable environment for both AEW and MCSs to grow and propagate. How the intensity and frequency of AEWs and MCSs will be affected in the changing climate is the topic of a follow-up study that will use the simulations introduced here. Additional future work will focus on longer and multiple future climate scenarios to asses whether the short-term changes in the weather-climate system of Africa presented here are representative of changes in long-term simulations or a consensus of climate model simulations.

Finally, we call upon communities whose livelihoods depend on water-fed crops to prepare and adapt for the possibility of more intense monsoonal rainfall extremes to be located near the Guinea Highlands, the Cameroon Mountains, and coastal countries sharing the Bight of Benin coast. Forecasting centers and risk management agencies should assess the impact and implication of such changes, and take the necessary actionable steps toward mitigating loss of life and property.

5 Open Research

Post-processed model outputs and the namelists for the MPAS-A simulations can be accessed at https://doi.org/10.5065/wfzv-nx43 (Núñez Ocasio & Dougherty, 2024). The modified MPAS-A code to output isobaric variables following MPAS developers can be found in the first author's Github: https://github.com/knubez/MPAS-Model. Please reference this paper that uses this code and/or the one mentioned on GitHub. The ERA5 (https://rda.ucar.edu/datasets/ds633.0/) and LENS2 (https://www.cesm.ucar.edu/community-projects/lens2) for initial and lateral boundary conditions were accessed via the NSF NCAR Research Data Archive via the Computational and Information Systems Laboratory (CISL).

Acknowledgments

Thank you to the NSF NCAR internal reviewer Chris Davis. We thank the reviewers. This work was completed while the first author held an NSF NCAR Advanced Study Program Postdoctoral Fellowship. This material is based upon work supported by the NSF National Center for Atmospheric Research, which is a major facility sponsored by the U.S. National Science Foundation under Cooperative Agreement No. 1852977. We acknowledge high-performance computing via Cheyenne (doi: 10.5065/D6RX99HX) and Derecho (https://doi.org/10.5065/qx9a-pg09) through the NSF NCAR Computational and Information Systems Laboratory.

References

Ban, N., Schmidli, J., & Schar, C. (2015). Heavy precipitation in a changing climate: Does short term summer precipitation increase faster? *Geophysical Research Letters*, *42*(4), 1165–1172. doi: 10.1002/2014GL062588

Bercos-Hickey, E., Nathan, T. R., & Chen, S.-H. (2020). On the Relationship between the African Easterly Jet, Saharan Mineral Dust Aerosols, and West African Precipitation. *Journal of Climate*, *33*(9), 3533-3546. doi: 10.1175/JCLI-D-18-0661.1

Bercos-Hickey, E., & Patricola, C. M. (2021, 6). Anthropogenic influences on the African easterly jet–African easterly wave system. *Climate Dynamics*, *57*(9-10). doi: 10.1007/s00382-021-05838-1

Bercos-Hickey, E., Patricola, C. M., Loring, B., & Collins, W. D. (2023). The Relationship Between African Easterly Waves and Tropical Cyclones in Historical and Future Climates in the HighResMIP-PRIMAVERA Simulations. *Journal of Geophysical Research: Atmospheres*, *128*(7), e2022JD037471. doi: 10.1029/2022JD037471

Brannan, A. L., & Martin, E. R. (2019). Future characteristics of African Easterly Wave tracks. *Climate Dynamics*, *52*(9-10), 5567-5584. doi: 10.1007/s00382-018-4465-z

Brogli, R., Heim, C., Mensch, J., Sørland, S. L., & Schär, C. (2023). The pseudo-global-warming (PGW) approach: methodology, software package PGW4ERA5 v1.1, validation, and sensitivity analyses. *Geoscientific Model Development*, *16*(3), 907–926. doi: 10.5194/gmd-16-907-2023

Cornforth, R. J., Hoskins, B. J., & Thorncroft, C. D. (2009). The impact of moist processes on the African easterly jet–African easterly wave system. *Quarterly Journal of the Royal Meteorological Society*, *135*(641), 894-913. doi: 10.1002/qj.414

Diallo, I., Sylla, M. B., Camara, M., & Gaye, A. T. (2013). Interannual variability of rainfall over the Sahel based on multiple regional climate models simulations. *Theoretical and Applied Climatology*, *113*(1-2), 351-362. doi: 10.1007/s00704-012-0791-y

Dougherty, E. M., Prein, A. F., Gutmann, E. D., & Newman, A. J. (2023). Future Simulated Changes in Central U.S. Mesoscale Convective System Rainfall Caused by Changes in Convective and Stratiform Structure. *Journal of Geophysical Research: Atmospheres*, *128*(4), e2022JD037537. doi: 10.1029/2022JD037537

Dougherty, E. M., & Rasmussen, K. L. (2020). Changes in Future Flash Flood–Producing Storms in the United States. *Journal of Hydrometeorology*, *21*(10), 2221-2236. doi: 10.1175/JHM-D-20-0014.1

Dougherty, E. M., Sherman, E., & Rasmussen, K. L. (2020). Future Changes in the Hydrologic Cycle Associated with Flood-Producing Storms in California. *Journal of Hydrometeorology*, *21*(11), 2607-2621. doi: 10.1175/JHM-D-20-0067.1

Grell, G. A., & Freitas, S. R. (2014). A scale and aerosol aware stochastic convective parameterization for weather and air quality modeling. *Atmospheric Chemistry and Physics*, *14*(10), 5233–5250. doi: 10.5194/acp-14-5233-2014

Hamilton, H. L., Núñez Ocasio, K. M., Evans, J. L., Young, G. S., & Fuentes, J. D.

(2020). Topographic Influence on the African Easterly Jet and African Easterly Wave Energetics. *Journal of Geophysical Research: Atmospheres*, *125*(8), e2019JD032138. doi: 10.1029/2019JD032138

Hamilton, H. L., Young, G. S., Evans, J. L., Fuentes, J. D., & Núñez Ocasio, K. M. (2017). The relationship between the Guinea Highlands and the West African offshore rainfall maximum. *Geophysical Research Letters*, *44*(2), 1158–1166. doi: 10.1002/2016GL071170

Hannah, W. M., & Aiyyer, A. (2017). Reduced African Easterly Wave Activity with Quadrupled CO2 in the Superparameterized CESM. *Journal of Climate*, *30*(20), 8253-8274. doi: 10.1175/JCLI-D-16-0822.1

Hartmann, D. L., & Larson, K. (2002). An important constraint on tropical cloud—Climate feedback. *Geophysical Research Letters*, *29*(20), 12-1–12-4. doi: 10.1029/2002GL015835

Heim, C., Leutwyler, D., & Schär, C. (2023). Application of the pseudo-global warming approach in a kilometer-resolution climate simulation of the tropics. *Journal of Geophysical Research: Atmospheres*, *128*, 1-24. doi: 10.1029/2022JD037958

Hersbach, H., Bell, B., Berrisford, P., Hirahara, S., Horányi, A., Muñoz-Sabater, J., ... Thépaut, J.-N. (2020). The ERA5 global reanalysis. *Quarterly Journal of the Royal Meteorological Society*, *146*(730), 1999–2049. doi: 10.1002/qj.3803

Hsieh, J.-S., & Cook, K. H. (2007). A Study of the Energetics of African Easterly Waves Using a Regional Climate Model. *Journal of the Atmospheric Sciences*, *64*(2), 421-440. doi: 10.1175/JAS3851.1

Huang, X., Swain, D. L., & Hall, A. D. (2020). Future precipitation increases from very high resolution ensemble downscaling of extreme atmospheric river storms in California. *Science Advances*, *6*(29), 1-13. doi: 10.1126/sciadv.aba1323

Iacono, M. J., Delamere, J. S., Mlawer, E. J., Shephard, M. W., Clough, S. A., & Collins, W. D. (2008). Radiative forcing by long-lived greenhouse gases: Calculations with the AER radiative transfer models. *Journal of Geophysical Research: Atmospheres*, *113*(D13). doi: 10.1029/2008JD009944

Janiga, M. A., & Thorncroft, C. D. (2013). Regional differences in the kinematic and thermodynamic structure of African Easterly Waves. *Quarterly Journal of the Royal Meteorological Society*, *139*(675), 1598-1614. doi: 10.1002/qj.2047

Jones, P. W. (1999). First- and Second-Order Conservative Remapping Schemes for Grids in Spherical Coordinates. *Monthly Weather Review*, *127*(9), 2204–2210. doi: 10.1175/1520-0493(1999)127⟨2204:FASOCR⟩2.0.CO;2

Kawase, H., Yoshikane, T., Hara, M., Kimura, F., Yasunari, T., & Ailikun, B. (2009). Intermodal variability of future changes in the baui rainband estimated by the pseudo global warming downscaling method. *Journal of Geophysical Research: Atmospheres*, *114*(D24), 1-14. doi: 10.1029/2009JD011803

Kebe, I., Diallo, I., Sylla, M. B., De Sales, F., & Diedhiou, A. (2020). Late 21st Century Projected Changes in the Relationship between Precipitation, African Easterly Jet, and African Easterly Waves. *Atmosphere*, *11*(4). doi: 10.3390/atmos11040353

Lackmann, G. M. (2013). The south-central U.S. flood of May 2010: Present and future. *Journal of Climate*, *26*(13), 4688–4709. doi: 10.1175/JCLI-D-12-00392.1

Landsea, C. W. (1993). A Climatology of Intense (or Major) Atlantic Hurricanes. *Monthly Weather Review*, *121*(6), 1703-1713. doi: 10.1175/1520-0493(1993)121⟨1703:ACOIMA⟩2.0.CO;2

Lau, W. K. M., & Kim, K.-M. (2015). Robust Hadley Circulation changes and increasing global dryness due to CO2 warming from CMIP5 model projections. *Proceedings of the National Academy of Sciences*, *112*(12), 3630–3635. doi: 10.1073/pnas.1418682112

Loriaux, J. M., Lenderink, G., Roode, S. R. D., & Siebesma, A. P. (2013). Understanding Convective Extreme Precipitation Scaling Using Observations and an Entraining Plume Model. *Journal of the Atmospheric Sciences*, *70*(11), 3641–3655. doi: 10.1175/JAS-D-12-0317.1

Mahoney, K., Alexander, M., Scott, J. D., & Barsugli, J. (2013). High-resolution downscaled simulations of warms-season ex- treme precipitation events in the Colorado Front Range under past and future climates. *Journal of Climate*, *26*(21), 8671–8689. doi: 10.1175/JCLI-D-12-00744.1

Nakanishi, M., & Niino, H. (2004). An Improved Mellor–Yamada Level-3 Model with Condensation Physics: Its Design and Verification. *Boundary-Layer Meteorology*, *112*, 1–31. doi: 10.1023/B:BOUN.0000020164.04146.98

Newell, R. E., & Kidson, J. W. (1984). African mean wind changes between sahelian wet and dry periods. *Journal of Climatology*, *4*(1), 27-33. doi: 10.1002/joc

.3370040103

Niu, G.-Y., Yang, Z.-L., Mitchell, K. E., Chen, F., Ek, M. B., Barlage, M., … Xia, Y. (2011). The community Noah land surface model with multiparameterization options (Noah-MP): 1. Model description and evaluation with local-scale measurements. *Journal of Geophysical Research: Atmospheres*, *116*(D12). doi: /10.1029/2010JD015139

Núñez Ocasio, K. M. (2023). MPAS-A moisture-sensitivity simulations with convection-permitting resolution and regional configuration using the Model for Prediction Across Scales (MPAS) version 7.3. *NCAR/UCAR - GDEX*. doi: 10.5065/gry9-7q56

Núñez Ocasio, K. M., Brammer, A., Evans, J. L., Young, G. S., & Moon, Z. L. (2021). Favorable Monsoon Environment over Eastern Africa for Subsequent Tropical Cyclogenesis of African Easterly Waves. *Journal of the Atmospheric Sciences*, *78*(9), 2911–2925. doi: 10.1175/JAS-D-20-0339.1

Núñez Ocasio, K. M., Davis, C. A., Moon, Z. L., & Lawton, Q. A. (2024). Moisture Sensitivity of the African Easterly Wave-African Easterly Jet and Convection Systems. , *in review for Journal of Advances in Modeling Earth Systems*.

Núñez Ocasio, K. M., & Dougherty, E. M. (2024). MPAS-A pseudo-global warming (PGW) experiment with convection-permitting resolution and regional configuration using the Model for Prediction Across Scales (MPAS) version 8.0.1. *NCAR/UCAR - GDEX*. doi: 10.5065/wfzv-nx43

Núñez Ocasio, K. M., Evans, J. L., & Young, G. S. (2020a). Tracking Mesoscale Convective Systems that are Potential Candidates for Tropical Cyclogenesis. *Monthly Weather Review*, *148*(2), 655-669. doi: 10.1175/MWR-D-19-0070.1

Núñez Ocasio, K. M., Evans, J. L., & Young, G. S. (2020b). A Wave-Relative Framework Analysis of AEW–MCS Interactions Leading to Tropical Cyclogenesis. *Monthly Weather Review*, *148*(11), 4657-4671. doi: 10.1175/MWR-D-20-0152.1

Núñez Ocasio, K. M., & Rios-Berrios, R. (2022). AEW hindcast using the Model for Prediction Across Scales-Atmosphere (MPAS-A) version 7.1. National Center for Atmospheric Research. [Dataset]. *NCAR/UCAR - GDEX*. doi: 10.5065/t224-6s94

Núñez Ocasio, K. M., & Rios-Berrios, R. (2023). African Easterly Wave Evolution and Tropical Cyclogenesis in a Pre-Helene (2006) Hindcast Using the Model for Prediction Across Scales-Atmosphere (MPAS-A). *Journal of Advances in Modeling Earth Systems*, *15*(2), e2022MS003181. doi: 10.1029/2022MS003181

Prein, A. F., Liu, C., Ikeda, K., Trier, S. B., Rasmussen, R. M., Holland, G. J., & Clark, M. P. (2017). Increased rainfall volume from future convective storms in the US. *Nature Climate Change*, *7*(12), 880–884. doi: 10.1038/s41558-017-0007-7

Pytharoulis, I., & Thorncroft, C. (1999). The Low-Level Structure of African Easterly Waves in 1995. *Monthly Weather Review*, *127*(10), 2266–2280. doi: 10.1175/1520-0493(1999)127⟨2266:TLLSOA⟩2.0.CO;2

Rajasree, V., Cao, X., Ramsay, H., Núñez Ocasio, K. M., Kilroy, G., Alvey, G. R., ... Yu, H. (2023). Tropical cyclogenesis: Controlling factors and physical mechanisms. *Tropical Cyclone Research and Review*, *12*(3), 165-181. doi: 10.1016/j.tcrr.2023.09.004

Rasmussen, K. L., Prein, A. F., Rasmussen, R. M., Ikeda, K., & Liu, C. (2020). Changes in the convective population and thermodynamic environments in convection-permitting regional climate simulations over the United States. *Climate Dynamics*, *55*, 383–408. doi: 10.1007/s00382-017-4000-7

Rodgers, K. B., Lee, S.-S., Rosenbloom, N., Timmermann, A., Danabasoglu, G., Deser, C., ... Yeager, S. G. (2021). Ubiquity of human-induced changes in climate variability. *Earth System Dynamics*, *12*(4), 1393–1411. doi: 10.5194/esd-12-1393-2021

Schär, C., Frei, C., Lüthi, D., & Davies, H. C. (1996). Surrogate climate-change scenarios for regional climate models. *Geophysical Research Letters*, *23*(6), 669-672. doi: 10.1029/96GL00265

Shaw, T. A., & Miyawaki, O. (2023). Fast upper-level jet stream winds get faster under climate change. *Nature Climate Change*, *14*, 61–67. doi: 10.1038/s41558-023-01884-1

Skamarock, W. C., Klemp, J. B., Duda, M. G., Fowler, L. D., Park, S.-H., & Ringler, T. D. (2012). A Multiscale Nonhydrostatic Atmospheric Model Using Centroidal Voronoi Tesselations and C-Grid Staggering. *Monthly Weather Review*, *140*(9), 3090–3105. doi: 10.1175/MWR-D-11-00215.1

Skinner, C. B., & Diffenbaugh, N. S. (2014). Projected changes in African easterly wave intensity and track in response to greenhouse forcing. *Proceedings of the National Academy of Sciences*, *111*(19), 6882-6887. doi: 10.1073/pnas.1319597111

Sylla, M. B., Diallo, I., & Pal, J. S. (2013). West African Monsoon in State-of-the-Science Regional Climate Models. In A. Tarhule (Ed.), *Climate variability* (chap. 1). Rijeka: IntechOpen. doi: 10.5772/55140

Thompson, G., Field, P. R., Rasmussen, R. M., & Hall, W. D. (2008). Explicit Forecasts of Winter Precipitation Using an Improved Bulk Microphysics Scheme. Part II: Implementation of a New Snow Parameterization. *Monthly Weather Review*, *136*(12), 5095–5115. doi: 10.1175/2008MWR2387.1

Tomassini, L., Parker, D. J., Stirling, A., Bain, C., Senior, C., & Milton, S. (2017). The interaction between moist diabatic processes and the atmospheric circulation in African Easterly Wave propagation. *Quarterly Journal of the Royal Meteorological Society*, *143*(709), 3207–3227. doi: 10.1002/qj.3173

Xu, K.-M., & Randall, D. A. (1996). A Semiempirical Cloudiness Parameterization for Use in Climate Models. *Journal of Atmospheric Sciences*, *53*(21), 3084–3102. doi: 10.1175/1520-0469(1996)053⟨3084:ASCPFU⟩2.0.CO;2

Zhang, G. (2023). Warming-induced contraction of tropical convection delays and reduces tropical cyclone formation. *Nat. Commun.*, *14*(1), 6274. doi: 10.1038/s41467-023-41911-5

Zipser, E. J., Twohy, C. H., Tsay, S.-C., Thornhill, K. L., Tanelli, S., Ross, R., … Anderson, B. (2009). The Saharan Air Layer and the Fate of African Easterly Waves—NASA's AMMA Field Study of Tropical Cyclogenesis. *Bulletin of the American Meteorological Society*, *90*(8), 1137–1156. doi: 10.1175/2009BAMS2728.1

The Effect of Pseudo-Global Warming on the Weather-Climate System of Africa in a Convection-Permitting Model

K. M. Núñez Ocasio[1], Erin M. Dougherty[1]

[1]NSF National Center for Atmospheric Research, Boulder, CO, USA

Key Points:

- The weather-climate system of Africa is explored with the novel use of a convection-permitting model and the pseudo-global warming method.
- The African easterly jet and areas of monsoon flow will intensify in a warming climate scenario together with increased monsoon moisture.
- An increase in precipitation is expected in a future warming climate scenario over the monsoon, high topography, and the eastern Atlantic.

Corresponding author: Kelly M. Núñez Ocasio, `knocasio@ucar.edu`

Abstract

The weather-climate system of Africa encompassing the African easterly jet (AEJ) and the West African Monsoon (WAM) can largely modulate high-impact weather over Africa and the tropical Atlantic. How the weather-climate system of Africa will change with a warming climate is just starting to be addressed due to global climate model limitations in resolving convection. We employ a novel atmospheric convection-permitting model regional setup alongside the pseudo-global warming (PGW) approach to address climate change impacts on the weather-climate system of Africa. Our findings indicate that the AEJ and areas of monsoon flow intensify in a future warming climate scenario together with an increase in monsoonal moisture. Moreover, precipitation will increase over high topography and shift southward due to a latitudinal expansion and increase of deep convection closer to the equator. This has relevant ramifications for the livelihood of communities that depend on water-fed crops in tropical Africa.

Plain Language Summary

The weather-climate system of Africa is closely linked to high-impact weather events, such as storms and African easterly waves, which can lead to tropical cyclones. Studying how the weather-climate system of Africa will change with a warming climate is a recent research focus. In our study, we use a novel weather model to investigate these changes. By adjusting the model to reflect a future warming climate scenario, we discover that the African easterly jet, convection, and West African Monsoon will become stronger. Additionally, rainfall will increase in the monsoonal region and shift southward. This information is vital, as it significantly affects communities relying on water-fed crops.

1 Introduction

The weather-climate system of Africa comprises of the African easterly jet (AEJ) sustaining African easterly waves (AEWs), the West African Monsoon (WAM), and associate convection. The AEJ arises from thermal wind balance over the northern summer months due to the very warm and dry Saharan desert over North Africa and the relatively cooler and moist conditions south of it (Pytharoulis & Thorncroft, 1999). The interactions between the AEJ and the WAM can dictate monsoonal precipitation patterns (Diallo et al., 2013; Sylla et al., 2013; Pytharoulis & Thorncroft, 1999; Hsieh & Cook, 2007; Bercos-Hickey et al., 2020), and the formation, growth, and propagation of mesoscale convective systems (MCSs) and AEWs which can serve as tropical cyclone (TC) precursors (Landsea, 1993; Núñez Ocasio et al., 2021, 2020b; Rajasree et al., 2023). Both AEWs and MCSs are high-impact weather events embedded within the complex African weather-climate system.

Few studies have specifically addressed how the AEJ-AEW system and WAM may change in a warming climate (Skinner & Diffenbaugh, 2014; Hannah & Aiyyer, 2017; Brannan & Martin, 2019; Kebe et al., 2020; Bercos-Hickey & Patricola, 2021; Bercos-Hickey et al., 2023). This is largely due to global climate models (GCMs) and regional models with deep convection parameterized not properly resolving the complex moisture-convective feedbacks and the multi-spatial nature of the weather-climate system of Africa (Cornforth et al., 2009; Janiga & Thorncroft, 2013; Tomassini et al., 2017; Núñez Ocasio et al., 2020a; Núñez Ocasio & Rios-Berrios, 2023).

For example, Kebe et al. (2020) found a future intensification and southern shift of the AEJ related to a shift in the meridional temperature gradient causing a decrease in AEW activity. Skinner and Diffenbaugh (2014) found an intensification of the meridional temperature gradient and the AEJ although they did not establish a consistent movement of the location of the jet. They also found an increase in low-level westerly flow beneath the jet and in AEW activity. Using a regional WRF configuration with a relatively coarse resolution of 27 km and parameterized convection, Bercos-Hickey and Patricola (2021) found that the AEJ weakens, shifts poleward, and is located at a higher altitude in the future climate with increased precipitation and low-level westerlies over the Sahel region. They also show an increase in the strength of the meridional temperature gradient. These results are similar to Núñez Ocasio et al. (2024) moisture sensitivity experiments except that they show that the AEJ is more intense in a moister environment. Noteworthy is that Núñez Ocasio et al. (2024) study uses a novel convection-permitting regional setup using the Model for Prediction Across Scales-Atmosphere (MPAS-A). Although moisture-sensitivity experiments like these cannot be directly related to climate projection experiments for which the role of temperature and anthropogenic sources are considered, the comparison can help elucidate the role of moist-convective processes in the weather-climate system of Africa and their connection to AEWs. These few studies present conflicting findings regarding the future trajectory of the AEJ, the meridional temperature gradient over North Africa, and, consequently, precipitation patterns, as well as the intensity and frequency of AEWs.

To capture the effect of thermodynamic changes due to anthropogenic-induced warming, this study applies a pseudo-global warming (PGW) method over a several day period of high-impact weather in Africa in convection-permitting simulations. The PGW method adds a perturbation representative of a future climate state to renanalysis data to understand how today's weather will change under warmer and moister conditions (Schär et al., 1996). While the PGW method has been applied in the mid-latitudes to study regional climate change impacts at convection-permitting scales on convection (Prein et al., 2017; Rasmussen et al., 2020; Dougherty et al., 2023), heavy rainfall (Schär et al., 1996; Kawase et al., 2009; Lackmann, 2013; Ban et al., 2015; Dougherty & Rasmussen, 2020), and atmospheric rivers (Mahoney et al., 2013; Dougherty et al., 2020), very few studies have utilized this approach to study climate change impacts on tropical precipitation, aside from Heim et al. (2023) and Bercos-Hickey and Patricola (2021). However, even studies that have applied the PGW method to the tropics use the WRF model, whereas this is the first study to apply it to the MPAS-A model.

Understanding how the weather-climate system of Africa evolves with climate change using convection-permitting modeling can enhance our ability to assess the critical implications of environments conducive to high-impact weather such as tropical cyclones and AEWs. This is the first study to the authors' knowledge that applies the PGW method to a Model for Prediction Across Scales-Atmosphere (MPAS-A) regional variable-resolution configuration introduced in Núñez Ocasio et al. (2024) that is capable of simulating processes at convection-permitting scales.

This study aims to answer the following scientific question:

Q: What are the short-term changes to the African weather-climate system in a future warmer climate scenario?

2 Methods and Data

2.1 MPAS Configuration

The Model for Prediction Across Scales-Atmosphere (MPAS-A) version 8.0.1 with the Limited-Area configuration was used for this study (Skamarock et al., 2012; Núñez Ocasio & Dougherty, 2024) to simulate the period of 1200 UTC 8 September–1800 UTC 13 September 2006 as in Núñez Ocasio and Rios-Berrios (2023); Núñez Ocasio et al. (2024).

Various features were active during this period including AEWs, MCSs, WAM, and ITCZ, all while during field campaigns NAMMA and AMMA (Zipser et al., 2009). In addition to initializing the model at 1200 UTC on 8 September, two other sets of experiments were completed: initializing the model at 00 UTC on 5 September and initializing at 00 UTC on 6 September. In incorporating three sets of experiments, we can account for spinup and the sensitivity to small perturbations for precipitation details given the short integration period.

The Limited-Area domain is from 30°S to 51°N and 65°W to 59°E depicted in Núñez Ocasio and Dougherty (2024)(and in Núñez Ocasio et al. (2024) their Figure 1). A 15-km–3-km variable-resolution mesh was used with the 3-km high-resolution refinement region elliptically shaped. The mesh was rotated over North Africa and the eastern Atlantic to ensure the track of AEWs and the inclusion of the ITCZ, AEJ, and WAM within the refined region.

The "convection permitting" physics suite was used here as in Núñez Ocasio et al. (2024). The scale-aware Grell-Freitas convection parameterization scheme (Grell & Freitas, 2014) changes from parameterized deep convection at the hydrostatic scales (parameterized grid is at 15 km) to only parameterize shallow convection in the refined 3-km region. At 3 km, deep convection was explicitly resolved. The rest of the schemes include RRTMG shortwave and longwave radiation (Iacono et al., 2008), Xu-Randall subgrid cloud fraction (Xu & Randall, 1996), MYNN boundary-layer and surface-layer schemes (Nakanishi & Niino, 2004), Noah land-surface scheme (Niu et al., 2011), and Thompson microphysics (Thompson et al., 2008).

The model was configured to run with 55 levels. Model outputs in the native unstructured grid were hourly. Native model output was vertically interpolated to obtain isobaric variables with 27 isolevels. The model output was spatially interpolated to a latitude and longitude grid equivalent of a 0.25°×0.25° horizontal resolution. The interpolation used a first-order conservative Gaussian grid (Jones, 1999) as done in Núñez Ocasio and Rios-Berrios (2022); Núñez Ocasio (2023).

2.2 Pseudo-global Warming Experiment

The ECMWF reanalysis 5th Generation (ERA5; Hersbach et al., 2020) was used to initiate the model and provide lateral boundary conditions hourly for the control (CTRL) simulations. The PGW experiments are the same as the CTRL experiments, except a delta signal representative of a future climate state is added to the ERA5 forcing data at the lateral boundaries:

$$CTRL = ERA5 \tag{1}$$

$$PGW = ERA5 + \Delta LENS2 \tag{2}$$

where Δ is given by the following:

$$\Delta = (2070 - 2100)\text{–}(1991 - 2021) \tag{3}$$

The PGW experiment takes the 100-member ensemble mean difference of the Community Earth System Model (CESM) Large Ensemble (LENS) version 2 (LENS2; Rodgers et al., 2021) at the end-of-century (2070-2100) under the SSP3-7.0 future radiative forcing scenario from the historical period (1991-2021). The perturbed variables from LENS2 added to ERA5 include temperature, geopotential height, horizontal winds, relative humidity, sea surface temperature, soil temperature, and pressure. Perturbing pressure, geopotential height, and winds, alongside temperature and humidity, ensure balance is maintained in the atmosphere (Brogli et al., 2023). This method thus simulates similar weather patterns as the current day but under warmer and moister conditions. Using the ensemble mean from LENS2 also assures that this response is a robust climate change signal, and not due to the internal variability of the model (Huang et al., 2020).

A limitation of the study is that it uses only one future projection scenario and one climate model for simulations of short integration time. Nonetheless, the main differences between the CTRL and PGW simulations in three experiments with different initializations are noteworthy and consistent across experiments, providing confidence that our results are not just artifacts of spin-up time. The variability across the three experiments initialized at different times is also noted in the study. This demonstrates that this kind of framework can be applied to multiple future climate scenarios and longer simulations. The objective of this study is on how future climate projections will affect the weather-climate system of Africa at short time scales, and thus, the focus is on a short period.

3 Results

To validate our regional convection-permitting PGW approach, we first assess the effects of the future warming on convection and precipitation associated with the ITCZ over the eastern Atlantic and the WAM over land. The differences across CTRL and PGW simulations (Figure 1g, Figure S1g, and Figure S2g) shows higher precipitation rates in the future climate. Specifically, precipitation rates are greater in the PGW scenario over the eastern Atlantic offshore waters (part of the ITCZ and West African offshore rainfall maximum), the Guinea Highlands, Cameroon Mountains, and the offshore waters of the Bight of Benin following the coast of Nigeria, Cameroon, Equatorial Guinea, and Gabon.

Although there is a slight increase in precipitation over the Sahel in the future climate agreeing with Bercos-Hickey and Patricola (2021) findings, the more prominent increases in precipitation here are located south of 10°N. Moisture-sensitivity experiments by Núñez Ocasio et al. (2024) also show these distinct peaks in precipitation over the region of the west African coast rainfall maximum, Guinea Highlands, and over the coast of the Bight of Benin with maxima over the Cameroon Mountains. The similarities across the PGW experiment here and moist-sensitivity experiments in Núñez Ocasio et al. (2024) may suggest a key role of water vapor in modulating future precipitation extreme patterns over the ITCZ and African monsoonal belt over tropical Africa.

With respect to the WAM, it is evident from Figure 1 (second column and in S1 and S2 for the additional experiments) that monsoonal moisture will increase in the future climate scenario both over land and water consistent with the increase in precipitation. There is variability across experiments on the location and intensity of the WAM confluent zone over the continent (Figure 1i, S1i, and S2i). However, the southwesterly monsoonal flow over the Gulf of Guinea and the embedded Bight of Benin consistently shows a strengthening across all experiments in the future climate. Over the western coast of Africa a prominent cyclonic feature also exhibits intensification in the future. This feature can be a signal of both intensifying AEWs and ITCZ.

Figure 2 (as well as S3 and S4) shows a time-average latitude analysis over a longitudinal average defined as the WAM box from 15°W to 25°E. More precipitable water content across the monsoonal region is to be expected in the future climate due to moisture increases following the Clausius-Clapeyron relationship and consistent with the

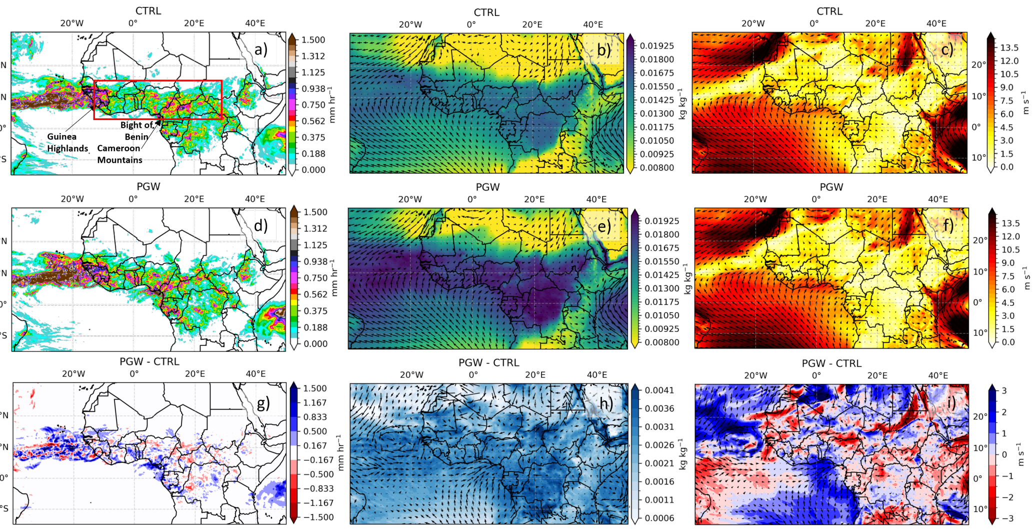

Figure 1. Time-averaged precipitation rates, 950-hPa water vapor mixing ratio (shade), and 950-hPA total winds (vectors and shade) removing the first 24 hours of the simulation for CTRL in (a), (b), and (c), respectively. The same from (d-f) for PGW and from (g-i) for the differences. Labels for Guinea Highlands, Bight of Benin, and the Cameroon Mountains are included in (a) for reference. The red square denotes the region that will be named WAM box hereon from 15°W to 25°E and 4°N to 15°N.

increase in monsoonal moisture (Figure 2; precipitable water). However, the average precipitation rate over the domain increases at less than the Clausius-Clapeyron rate of 7 % K^{-1}, with an increase of 4.8 % K^{-1}. This rate of increase is possible because we consider all precipitation, not just precipitation extremes or convection specifically, where precipitation rates are expected to increase at or above the Clausius-Clapeyron rate (Prein et al., 2017; Loriaux et al., 2013).

Convection is also deeper between 5°S and 7.5°N (Figure 2; OLR) in the future climate. Related to the deeper ITCZ and monsoonal convection in the PGW scenario, regions of peak precipitation rates are to expected to have even higher rates and the peaks will be shifted equatorward (Figure 2; precipitation rates) as was evident from Figure 1. Heim et al. (2023) similarly saw a southward shift in the precipitation maximum near the equator and intensification of the ITCZ.

Cross sections of time-average diabatic heating rates show where the maximum of moist convection for each simulation is located (Figure 3, and S5). The majority of the

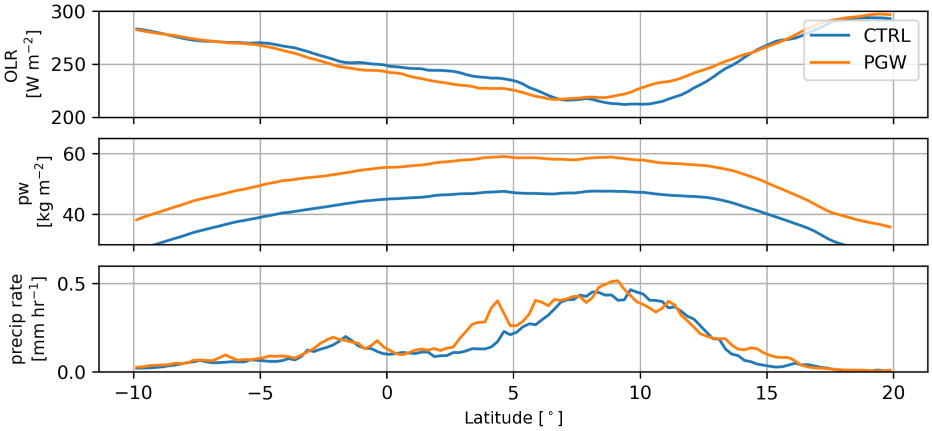

Figure 2. Latitude analyses of time-averaged, zonally averaged (top) OLR, (middle) precipitable water (pw), and (bottom) precipitation rate removing the first 24 hours of the simulation for CTRL (blue lines) and PGW (orange lines). Longitude average is taken for the WAM box.

monsoonal moist convection is located between 5°N and 15°N in the CTRL scenario with maximum between 10°N and 12°N. The future scenario exhibits a latitudinal expansion of the convection with deeper (top-heavy signature reaching above 250 hPa). Although there is variability across experiments as to where the maximum of diabatic heating difference lies (compare maxima locations in Figure 3c, S5c, and S5f) there is consistency across experimenters that deeper and more intense convection shifts to the south of 10°N in the PGW simulations. This diabatic heating signature agrees with the expected southward shift of the ITCZ and monsoonal precipitation shown in the previous figures.

Such a deepening of diabatic heating is expected in a warmer climate in the tropics, fitting with the fixed anvil temperature (FAT) hypothesis (Hartmann & Larson, 2002), whereby anvils rise in a warmer climate and thereby remain at the same temperature. Interestingly, the widening of diabatic heating contrasts the idea of a “deep-tropics squeeze” (Lau & Kim, 2015) that suggests a narrowing of the ITCZ. Similar to this idea is the “warming-induced contraction of tropical convection” hypothesis by a GCM climate change study over the tropics (Zhang, 2023), though the PGW convection-permitting simulations from Heim et al. (2023) also do not find such a pronounced narrowing of the ITCZ.

Within the weather-climate system of Africa is the AEJ which serves as an energy source for both AEWs and MCSs and plays a major role in dictating the high-impact weather over the region. Previous climatology studies have shown that the AEJ is weaker

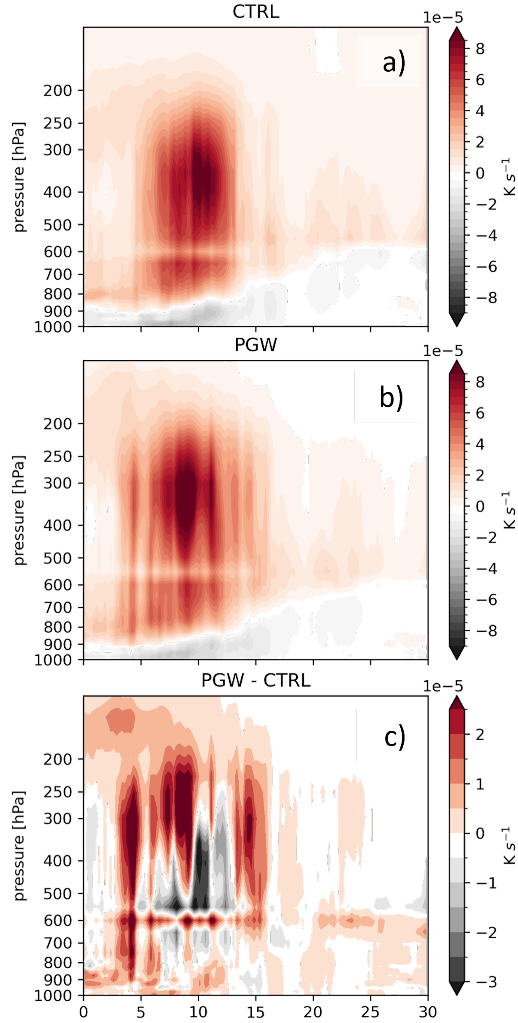

Figure 3. Vertical cross-section of the time-averaged diabatic heating rates from microphysics scheme removing the first 24 hours of the simulation for (a) CTRL, (b) PGW, and (c) the difference. Longitude average taken for WAM box. Y axis is in log scale.

and farther north during wet years (Newell & Kidson, 1984; Sylla et al., 2013; Diallo et al., 2013; Bercos-Hickey et al., 2020). In Bercos-Hickey and Patricola (2021) they found a weaker, more northward-positioned AEJ located at a higher altitude in the future climate. Similarly, the difference between PGW and CTRL here in Figure 4c (as well as in S6e and S7e) show an AEJ shifted northward in the future climate with core greater than 13 m s^{-1} located at or slightly above 15°N at 600 hPa. However, unlike Bercos-Hickey and Patricola (2021), the core of the AEJ here is more intense in the future scenario than the CTRL experiment. A stronger more northward AEJ and wetter conditions were also found in Núñez Ocasio et al. (2024) moisture-sensitivity experiments al-luding again to the role of water vapor on high-impact weather events. With the AEJ strengthening and being positioned more northward relative to the WAM confluent zone over the continent in the future climate, is less likely for the AEJ to interact with the southwesterly monsoonal flow sufficiently. This is turn inhibits significant shear production and limits the likelihood of barotropic and baroclinic energy exchanges ultimately, affecting the intensity of AEWs and the AEJ-AEW system (i.e., Núñez Ocasio et al., 2024). How the AEJ-AEW system, as well as how the intensity and frequency of AEWs and MCSs will be affected in the changing climate is out scope of this study. However, it is currently being explored and is the topic of a follow-up study.

At the larger scales, the upper-level jets such as the tropical easterly jet (TEJ) with a maximum of around 250 hPa will strengthen while the subtropical jet with the core at about 200 hPa, will weaken in the future climate scenario. The strengthening of the AEJ in the future climate scenario is related to the low-level meridional potential temperature gradient. Additionally, the stronger TEJ is consistent with a strengthening of jet stream wind projected by GCMs globally, due to an increase in the meridional humidity gradient under climate change that impacts the thermal wind via density gradients (Shaw & Miyawaki, 2023).

Within the weather-climate system of Africa, the meridional temperature gradient during the northern summer months gives rise to the AEJ through thermal wind balance. Skinner and Diffenbaugh (2014) and Bercos-Hickey and Patricola (2021) found an increase in the strength of the meridional temperature gradient. Agreeing with these studies, it is evident that in the future climate scenario here, the strength of the meridional potential temperature gradient increases across the atmospheric column (Figure 4f, S6f, and S7f). This stronger meridional potential temperature gradient relates to an increase in precipitation and monsoon intensity. The stronger meridional potential temperature gradient at the surface directly relates to the meridional potential vorticity (PV) reversal at the mid-levels that exists over the African continent during the northern summer months and satisfies the Charney-Stern criterion for dynamical instability (Pytharoulis & Thorncroft, 1999). This PV meridional gradient is also strengthened in the PGW scenario (not shown). Finally, given the evident increase in precipitation over high topography shown here in the future climate, it is noteworthy that topography like the Cameroon Mountains and the Guinea Highlands can influence the low-level meridional potential temperature gradient over Africa. This, in turn, can affect precipitation as we see here and AEW energetics (i.e., Hamilton et al., 2020, 2017).

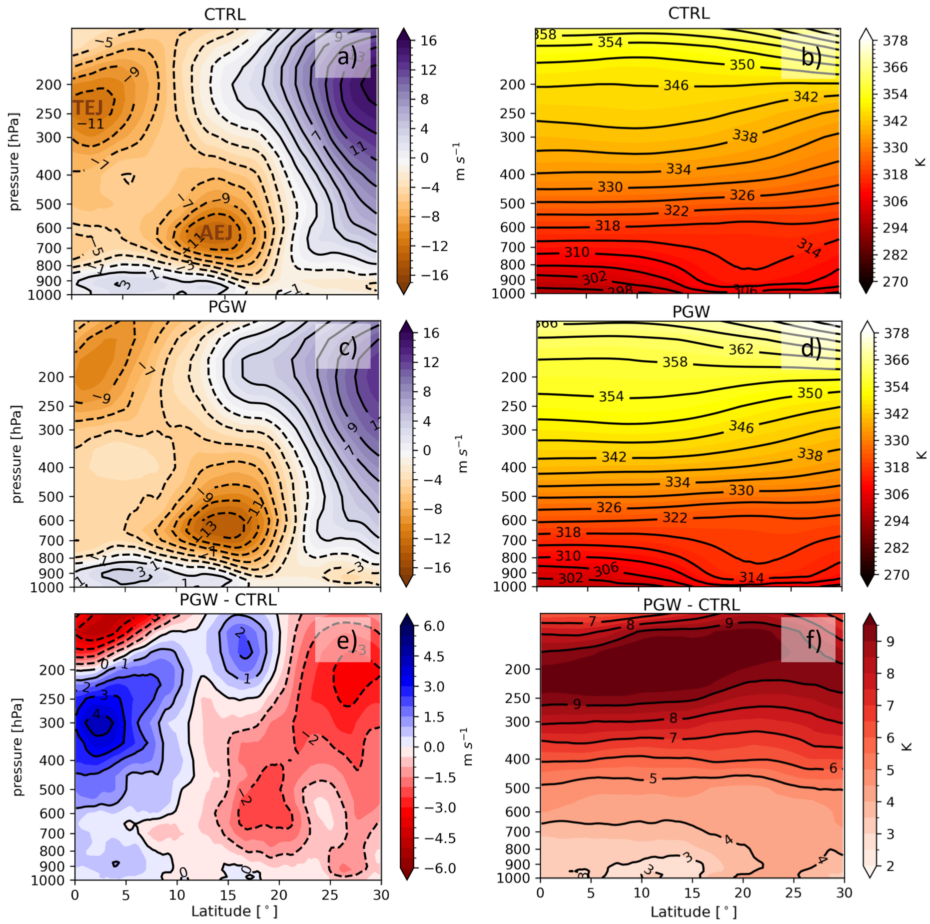

Figure 4. Vertical cross-section of the time-averaged zonal wind and potential temperature removing the first 24 hours of the simulation for CTRL in (a) and (b), respectively. The same from (c-d) for PGW, and from (e-f) for the differences. Longitude average taken for the WAM box. Y axis is in log scale. The AEJ and TEJ are labeled in (a).

4 Conclusions

Through a novel convection-permitting framework that applies the PGW method, we have addressed the question of what are the short-term changes to the weather-climate system of Africa in a future warming climate scenario.Using a convection-permitting model alongside the PGW method, we can better asses climate changes in a more realistic model setup to be able to compare our results to past studies that used GCMs and/or parameterized convection.

Although some variability is evident across the three experiments initialized at different times while using the same future climate scenario, consistent patterns emerge of how the weather-climate system of Africa will change with the changing climate. Different from past studies we find that the AEJ intensifies and shifts poleward in the future climate scenario. The ITCZ over the eastern Atlantic will intensify in a future climate scenario. An increase in precipitation rates related to a monsoonal increase in moisture is also to be expected in the future climate, especially south of 10°N. This southern shift of the precipitation is consistent with deeper and more intense convection shifting to the south of 10°N. In the future climate scenario, the southwesterly monsoonal flow over the Gulf of Guinea and the embedded Bight of Benin intensifies. Agreeing with past studies, we show an increase in the strength of the meridional temperature gradient. This strengthening is related to the intensification of both the AEJ at the mid-levels and of the TEJ.

The AEJ serves as an energy source for AEWs, and the WAM and ITCZ provide a moisture-favorable environment for both AEW and MCSs to grow and propagate. How the intensity and frequency of AEWs and MCSs will be affected in the changing climate is the topic of a follow-up study that will use the simulations introduced here. Additional future work will focus on longer and multiple future climate scenarios to asses whether the short-term changes in the weather-climate system of Africa presented here are representative of changes in long-term simulations or a consensus of climate model simulations.

Finally, we call upon communities whose livelihoods depend on water-fed crops to prepare and adapt for the possibility of more intense monsoonal rainfall extremes to be located near the Guinea Highlands, the Cameroon Mountains, and coastal countries sharing the Bight of Benin coast. Forecasting centers and risk management agencies should assess the impact and implication of such changes, and take the necessary actionable steps toward mitigating loss of life and property.

5 Open Research

Post-processed model outputs and the namelists for the MPAS-A simulations can be accessed at https://doi.org/10.5065/wfzv-nx43 (Núñez Ocasio & Dougherty, 2024). The modified MPAS-A code to output isobaric variables following MPAS developers can be found in the first author's Github: https://github.com/knubez/MPAS-Model. Please reference this paper that uses this code and/or the one mentioned on GitHub. The ERA5 (https://rda.ucar.edu/datasets/ds633.0/) and LENS2 (https://www.cesm.ucar.edu/community-projects/lens2) for initial and lateral boundary conditions were accessed via the NSF NCAR Research Data Archive via the Computational and Information Systems Laboratory (CISL).

Acknowledgments

Thank you to the NSF NCAR internal reviewer Chris Davis. We thank the reviewers. This work was completed while the first author held an NSF NCAR Advanced Study Program Postdoctoral Fellowship. This material is based upon work supported by the NSF National Center for Atmospheric Research, which is a major facility sponsored by the U.S. National Science Foundation under Cooperative Agreement No. 1852977. We acknowledge high-performance computing via Cheyenne (doi: 10.5065/D6RX99HX) and Derecho (https://doi.org/10.5065/qx9a-pg09) through the NSF NCAR Computational and Information Systems Laboratory.

References

Ban, N., Schmidli, J., & Schar, C. (2015). Heavy precipitation in a changing climate: Does short term summer precipitation increase faster? *Geophysical Research Letters*, *42*(4), 1165–1172. doi: 10.1002/2014GL062588

Bercos-Hickey, E., Nathan, T. R., & Chen, S.-H. (2020). On the Relationship between the African Easterly Jet, Saharan Mineral Dust Aerosols, and West African Precipitation. *Journal of Climate*, *33*(9), 3533-3546. doi: 10.1175/JCLI-D-18-0661.1

Bercos-Hickey, E., & Patricola, C. M. (2021, 6). Anthropogenic influences on the African easterly jet–African easterly wave system. *Climate Dynamics*, *57*(9-10). doi: 10.1007/s00382-021-05838-1

Bercos-Hickey, E., Patricola, C. M., Loring, B., & Collins, W. D. (2023). The Relationship Between African Easterly Waves and Tropical Cyclones in Historical and Future Climates in the HighResMIP-PRIMAVERA Simulations. *Journal of Geophysical Research: Atmospheres*, *128*(7), e2022JD037471. doi: 10.1029/2022JD037471

Brannan, A. L., & Martin, E. R. (2019). Future characteristics of African Easterly Wave tracks. *Climate Dynamics*, *52*(9-10), 5567-5584. doi: 10.1007/s00382-018-4465-z

Brogli, R., Heim, C., Mensch, J., Sørland, S. L., & Schär, C. (2023). The pseudo-global-warming (PGW) approach: methodology, software package PGW4ERA5 v1.1, validation, and sensitivity analyses. *Geoscientific Model Development*, *16*(3), 907–926. doi: 10.5194/gmd-16-907-2023

Cornforth, R. J., Hoskins, B. J., & Thorncroft, C. D. (2009). The impact of moist processes on the African easterly jet–African easterly wave system. *Quarterly Journal of the Royal Meteorological Society*, *135*(641), 894-913. doi: 10.1002/qj.414

Diallo, I., Sylla, M. B., Camara, M., & Gaye, A. T. (2013). Interannual variability of rainfall over the Sahel based on multiple regional climate models simulations. *Theoretical and Applied Climatology*, *113*(1-2), 351-362. doi: 10.1007/s00704-012-0791-y

Dougherty, E. M., Prein, A. F., Gutmann, E. D., & Newman, A. J. (2023). Future Simulated Changes in Central U.S. Mesoscale Convective System Rainfall Caused by Changes in Convective and Stratiform Structure. *Journal of Geophysical Research: Atmospheres*, *128*(4), e2022JD037537. doi: 10.1029/2022JD037537

Dougherty, E. M., & Rasmussen, K. L. (2020). Changes in Future Flash Flood–Producing Storms in the United States. *Journal of Hydrometeorology*, *21*(10), 2221-2236. doi: 10.1175/JHM-D-20-0014.1

Dougherty, E. M., Sherman, E., & Rasmussen, K. L. (2020). Future Changes in the Hydrologic Cycle Associated with Flood-Producing Storms in California. *Journal of Hydrometeorology*, *21*(11), 2607-2621. doi: 10.1175/JHM-D-20-0067.1

Grell, G. A., & Freitas, S. R. (2014). A scale and aerosol aware stochastic convective parameterization for weather and air quality modeling. *Atmospheric Chemistry and Physics*, *14*(10), 5233–5250. doi: 10.5194/acp-14-5233-2014

Hamilton, H. L., Núñez Ocasio, K. M., Evans, J. L., Young, G. S., & Fuentes, J. D.

(2020). Topographic Influence on the African Easterly Jet and African Easterly Wave Energetics. *Journal of Geophysical Research: Atmospheres*, *125*(8), e2019JD032138. doi: 10.1029/2019JD032138

Hamilton, H. L., Young, G. S., Evans, J. L., Fuentes, J. D., & Núñez Ocasio, K. M. (2017). The relationship between the Guinea Highlands and the West African offshore rainfall maximum. *Geophysical Research Letters*, *44*(2), 1158–1166. doi: 10.1002/2016GL071170

Hannah, W. M., & Aiyyer, A. (2017). Reduced African Easterly Wave Activity with Quadrupled CO2 in the Superparameterized CESM. *Journal of Climate*, *30*(20), 8253-8274. doi: 10.1175/JCLI-D-16-0822.1

Hartmann, D. L., & Larson, K. (2002). An important constraint on tropical cloud—Climate feedback. *Geophysical Research Letters*, *29*(20), 12-1–12-4. doi: 10.1029/2002GL015835

Heim, C., Leutwyler, D., & Schär, C. (2023). Application of the pseudo-global warming approach in a kilometer-resolution climate simulation of the tropics. *Journal of Geophysical Research: Atmospheres*, *128*, 1-24. doi: 10.1029/2022JD037958

Hersbach, H., Bell, B., Berrisford, P., Hirahara, S., Horányi, A., Muñoz-Sabater, J., … Thépaut, J.-N. (2020). The ERA5 global reanalysis. *Quarterly Journal of the Royal Meteorological Society*, *146*(730), 1999–2049. doi: 10.1002/qj.3803

Hsieh, J.-S., & Cook, K. H. (2007). A Study of the Energetics of African Easterly Waves Using a Regional Climate Model. *Journal of the Atmospheric Sciences*, *64*(2), 421-440. doi: 10.1175/JAS3851.1

Huang, X., Swain, D. L., & Hall, A. D. (2020). Future precipitation increases from very high resolution ensemble downscaling of extreme atmospheric river storms in California. *Science Advances*, *6*(29), 1-13. doi: 10.1126/sciadv.aba1323

Iacono, M. J., Delamere, J. S., Mlawer, E. J., Shephard, M. W., Clough, S. A., & Collins, W. D. (2008). Radiative forcing by long-lived greenhouse gases: Calculations with the AER radiative transfer models. *Journal of Geophysical Research: Atmospheres*, *113*(D13). doi: 10.1029/2008JD009944

Janiga, M. A., & Thorncroft, C. D. (2013). Regional differences in the kinematic and thermodynamic structure of African Easterly Waves. *Quarterly Journal of the Royal Meteorological Society*, *139*(675), 1598-1614. doi: 10.1002/qj.2047

Jones, P. W. (1999). First- and Second-Order Conservative Remapping Schemes for Grids in Spherical Coordinates. *Monthly Weather Review*, *127*(9), 2204–2210. doi: 10.1175/1520-0493(1999)127⟨2204:FASOCR⟩2.0.CO;2

Kawase, H., Yoshikane, T., Hara, M., Kimura, F., Yasunari, T., & Ailikun, B. (2009). Intermodal variability of future changes in the baui rainband estimated by the pseudo global warming downscaling method. *Journal of Geophysical Research: Atmospheres*, *114*(D24), 1-14. doi: 10.1029/2009JD011803

Kebe, I., Diallo, I., Sylla, M. B., De Sales, F., & Diedhiou, A. (2020). Late 21st Century Projected Changes in the Relationship between Precipitation, African Easterly Jet, and African Easterly Waves. *Atmosphere*, *11*(4). doi: 10.3390/atmos11040353

Lackmann, G. M. (2013). The south-central U.S. flood of May 2010: Present and future. *Journal of Climate*, *26*(13), 4688–4709. doi: 10.1175/JCLI-D-12-00392.1

Landsea, C. W. (1993). A Climatology of Intense (or Major) Atlantic Hurricanes. *Monthly Weather Review*, *121*(6), 1703-1713. doi: 10.1175/1520-0493(1993)121⟨1703:ACOIMA⟩2.0.CO;2

Lau, W. K. M., & Kim, K.-M. (2015). Robust Hadley Circulation changes and increasing global dryness due to CO2 warming from CMIP5 model projections. *Proceedings of the National Academy of Sciences*, *112*(12), 3630–3635. doi: 10.1073/pnas.1418682112

Loriaux, J. M., Lenderink, G., Roode, S. R. D., & Siebesma, A. P. (2013). Understanding Convective Extreme Precipitation Scaling Using Observations and an Entraining Plume Model. *Journal of the Atmospheric Sciences*, *70*(11), 3641–3655. doi: 10.1175/JAS-D-12-0317.1

Mahoney, K., Alexander, M., Scott, J. D., & Barsugli, J. (2013). High-resolution downscaled simulations of warms-season ex- treme precipitation events in the Colorado Front Range under past and future climates. *Journal of Climate*, *26*(21), 8671–8689. doi: 10.1175/JCLI-D-12-00744.1

Nakanishi, M., & Niino, H. (2004). An Improved Mellor–Yamada Level-3 Model with Condensation Physics: Its Design and Verification. *Boundary-Layer Meteorology*, *112*, 1–31. doi: 10.1023/B:BOUN.0000020164.04146.98

Newell, R. E., & Kidson, J. W. (1984). African mean wind changes between sahelian wet and dry periods. *Journal of Climatology*, *4*(1), 27-33. doi: 10.1002/joc

.3370040103

Niu, G.-Y., Yang, Z.-L., Mitchell, K. E., Chen, F., Ek, M. B., Barlage, M., ... Xia, Y. (2011). The community Noah land surface model with multiparameterization options (Noah-MP): 1. Model description and evaluation with local-scale measurements. *Journal of Geophysical Research: Atmospheres*, *116*(D12). doi: /10.1029/2010JD015139

Núñez Ocasio, K. M. (2023). MPAS-A moisture-sensitivity simulations with convection-permitting resolution and regional configuration using the Model for Prediction Across Scales (MPAS) version 7.3. *NCAR/UCAR - GDEX*. doi: 10.5065/gry9-7q56

Núñez Ocasio, K. M., Brammer, A., Evans, J. L., Young, G. S., & Moon, Z. L. (2021). Favorable Monsoon Environment over Eastern Africa for Subsequent Tropical Cyclogenesis of African Easterly Waves. *Journal of the Atmospheric Sciences*, *78*(9), 2911–2925. doi: 10.1175/JAS-D-20-0339.1

Núñez Ocasio, K. M., Davis, C. A., Moon, Z. L., & Lawton, Q. A. (2024). Moisture Sensitivity of the African Easterly Wave-African Easterly Jet and Convection Systems. , *in review for Journal of Advances in Modeling Earth Systems*.

Núñez Ocasio, K. M., & Dougherty, E. M. (2024). MPAS-A pseudo-global warming (PGW) experiment with convection-permitting resolution and regional configuration using the Model for Prediction Across Scales (MPAS) version 8.0.1. *NCAR/UCAR - GDEX*. doi: 10.5065/wfzv-nx43

Núñez Ocasio, K. M., Evans, J. L., & Young, G. S. (2020a). Tracking Mesoscale Convective Systems that are Potential Candidates for Tropical Cyclogenesis. *Monthly Weather Review*, *148*(2), 655-669. doi: 10.1175/MWR-D-19-0070.1

Núñez Ocasio, K. M., Evans, J. L., & Young, G. S. (2020b). A Wave-Relative Framework Analysis of AEW–MCS Interactions Leading to Tropical Cyclogenesis. *Monthly Weather Review*, *148*(11), 4657-4671. doi: 10.1175/MWR-D-20-0152.1

Núñez Ocasio, K. M., & Rios-Berrios, R. (2022). AEW hindcast using the Model for Prediction Across Scales-Atmosphere (MPAS-A) version 7.1. National Center for Atmospheric Research. [Dataset]. *NCAR/UCAR - GDEX*. doi: 10.5065/t224-6s94

Núñez Ocasio, K. M., & Rios-Berrios, R. (2023). African Easterly Wave Evolution and Tropical Cyclogenesis in a Pre-Helene (2006) Hindcast Using the Model for Prediction Across Scales-Atmosphere (MPAS-A). *Journal of Advances in Modeling Earth Systems*, *15*(2), e2022MS003181. doi: 10.1029/2022MS003181

Prein, A. F., Liu, C., Ikeda, K., Trier, S. B., Rasmussen, R. M., Holland, G. J., & Clark, M. P. (2017). Increased rainfall volume from future convective storms in the US. *Nature Climate Change*, *7*(12), 880–884. doi: 10.1038/s41558-017-0007-7

Pytharoulis, I., & Thorncroft, C. (1999). The Low-Level Structure of African Easterly Waves in 1995. *Monthly Weather Review*, *127*(10), 2266–2280. doi: 10.1175/1520-0493(1999)127⟨2266:TLLSOA⟩2.0.CO;2

Rajasree, V., Cao, X., Ramsay, H., Núñez Ocasio, K. M., Kilroy, G., Alvey, G. R., ... Yu, H. (2023). Tropical cyclogenesis: Controlling factors and physical mechanisms. *Tropical Cyclone Research and Review*, *12*(3), 165-181. doi: 10.1016/j.tcrr.2023.09.004

Rasmussen, K. L., Prein, A. F., Rasmussen, R. M., Ikeda, K., & Liu, C. (2020). Changes in the convective population and thermodynamic environments in convection-permitting regional climate simulations over the United States. *Climate Dynamics*, *55*, 383–408. doi: 10.1007/s00382-017-4000-7

Rodgers, K. B., Lee, S.-S., Rosenbloom, N., Timmermann, A., Danabasoglu, G., Deser, C., ... Yeager, S. G. (2021). Ubiquity of human-induced changes in climate variability. *Earth System Dynamics*, *12*(4), 1393–1411. doi: 10.5194/esd-12-1393-2021

Schär, C., Frei, C., Lüthi, D., & Davies, H. C. (1996). Surrogate climate-change scenarios for regional climate models. *Geophysical Research Letters*, *23*(6), 669-672. doi: 10.1029/96GL00265

Shaw, T. A., & Miyawaki, O. (2023). Fast upper-level jet stream winds get faster under climate change. *Nature Climate Change*, *14*, 61–67. doi: 10.1038/s41558-023-01884-1

Skamarock, W. C., Klemp, J. B., Duda, M. G., Fowler, L. D., Park, S.-H., & Ringler, T. D. (2012). A Multiscale Nonhydrostatic Atmospheric Model Using Centroidal Voronoi Tesselations and C-Grid Staggering. *Monthly Weather Review*, *140*(9), 3090–3105. doi: 10.1175/MWR-D-11-00215.1

Skinner, C. B., & Diffenbaugh, N. S. (2014). Projected changes in African easterly wave intensity and track in response to greenhouse forcing. *Proceedings of the National Academy of Sciences*, *111*(19), 6882-6887. doi: 10.1073/pnas.1319597111

Sylla, M. B., Diallo, I., & Pal, J. S. (2013). West African Monsoon in State-of-the-Science Regional Climate Models. In A. Tarhule (Ed.), *Climate variability* (chap. 1). Rijeka: IntechOpen. doi: 10.5772/55140

Thompson, G., Field, P. R., Rasmussen, R. M., & Hall, W. D. (2008). Explicit Forecasts of Winter Precipitation Using an Improved Bulk Microphysics Scheme. Part II: Implementation of a New Snow Parameterization. *Monthly Weather Review*, *136*(12), 5095–5115. doi: 10.1175/2008MWR2387.1

Tomassini, L., Parker, D. J., Stirling, A., Bain, C., Senior, C., & Milton, S. (2017). The interaction between moist diabatic processes and the atmospheric circulation in African Easterly Wave propagation. *Quarterly Journal of the Royal Meteorological Society*, *143*(709), 3207–3227. doi: 10.1002/qj.3173

Xu, K.-M., & Randall, D. A. (1996). A Semiempirical Cloudiness Parameterization for Use in Climate Models. *Journal of Atmospheric Sciences*, *53*(21), 3084–3102. doi: 10.1175/1520-0469(1996)053⟨3084:ASCPFU⟩2.0.CO;2

Zhang, G. (2023). Warming-induced contraction of tropical convection delays and reduces tropical cyclone formation. *Nat. Commun.*, *14*(1), 6274. doi: 10.1038/s41467-023-41911-5

Zipser, E. J., Twohy, C. H., Tsay, S.-C., Thornhill, K. L., Tanelli, S., Ross, R., … Anderson, B. (2009). The Saharan Air Layer and the Fate of African Easterly Waves—NASA's AMMA Field Study of Tropical Cyclogenesis. *Bulletin of the American Meteorological Society*, *90*(8), 1137–1156. doi: 10.1175/2009BAMS2728.1

Supporting Information for "The Effect of Pseudo-Global Warming on the Weather-Climate System of Africa in a Convection-Permitting Model"

K. M. Núñez Ocasio[1], Erin M. Dougherty[1]

[1]NSF National Center for Atmospheric Research, Boulder, CO, USA

Contents of this file

1. Figures S1 to S7

Introduction

This supporting information includes figures of the analysis for the additional CTRL and PGW model runs initialized on 00 UTC, 5 September 2006 and 00 UTC, 6 September 2006.

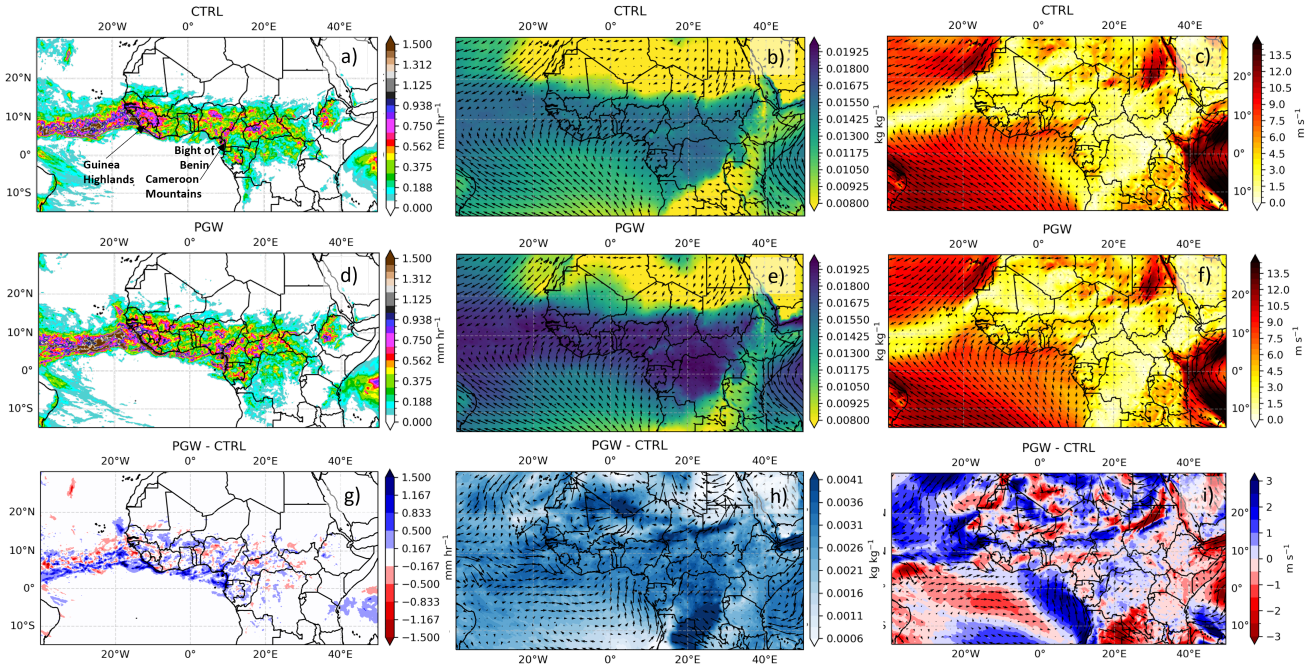

Figure S1. Time-averaged precipitation rates, 950-hPa water vapor mixing ratio (shade), and 950-hPA total winds (vectors and shade) initialized on 00 UTC, 5 September 2006 removing the first 24 hours of the simulation for CTRL in (a), (b), and (c), respectively. The same from (d-f) for PGW and from (g-i) for the differences. Labels for Guinea Highlands, Bight of Benin, and the Cameroon Mountains are included in (a) for reference.

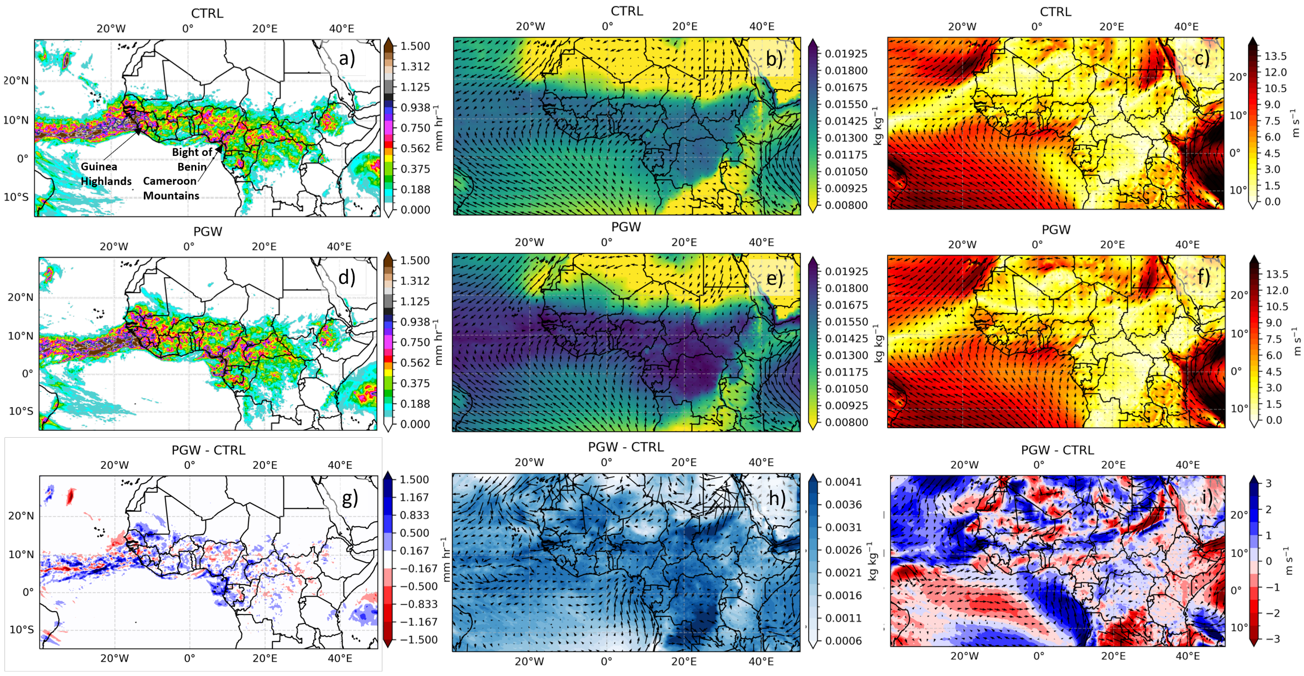

Figure S2. Time-averaged precipitation rates, 950-hPa water vapor mixing ratio (shade), and 950-hPA total winds (vectors and shade) initialized on 00 UTC, 6 September 2006 removing the first 24 hours of the simulation for CTRL in (a), (b), and (c), respectively. The same from (d-f) for PGW and from (g-i) for the differences. Labels for Guinea Highlands, Bight of Benin, and the Cameroon Mountains are included in (a) for reference.

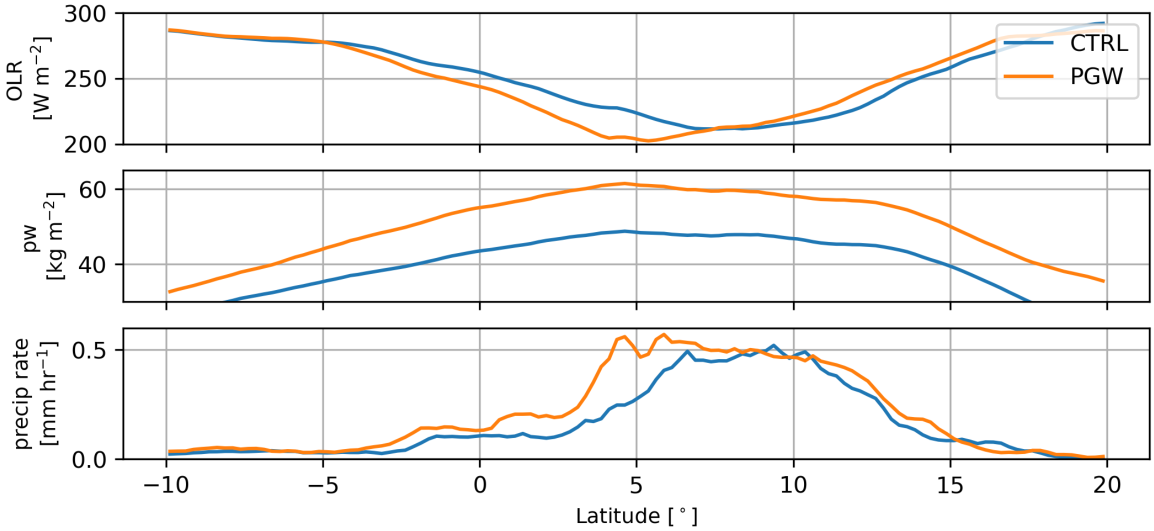

Figure S3. Latitude analyses of time-averaged, zonally averaged (top) OLR, (middle) precipitable water (pw), and (bottom) precipitation rate initialized on 00 UTC, 5 September 2006 removing the first 24 hours of the simulation for CTRL (blue lines) and PGW (orange lines). Longitude average taken for the WAM box.

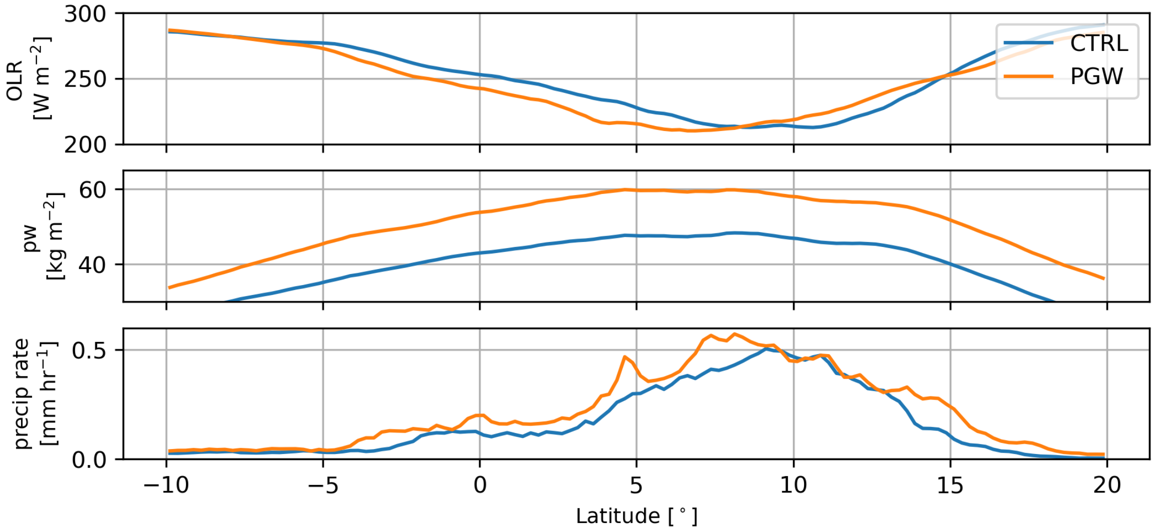

Figure S4. Latitude analyses of time-averaged, zonally averaged (top) OLR, (middle) precipitable water (pw), and (bottom) precipitation rate initialized on 00 UTC, 6 September 2006 removing the first 24 hours of the simulation for CTRL (blue lines) and PGW (orange lines). Longitude average taken for the WAM box.

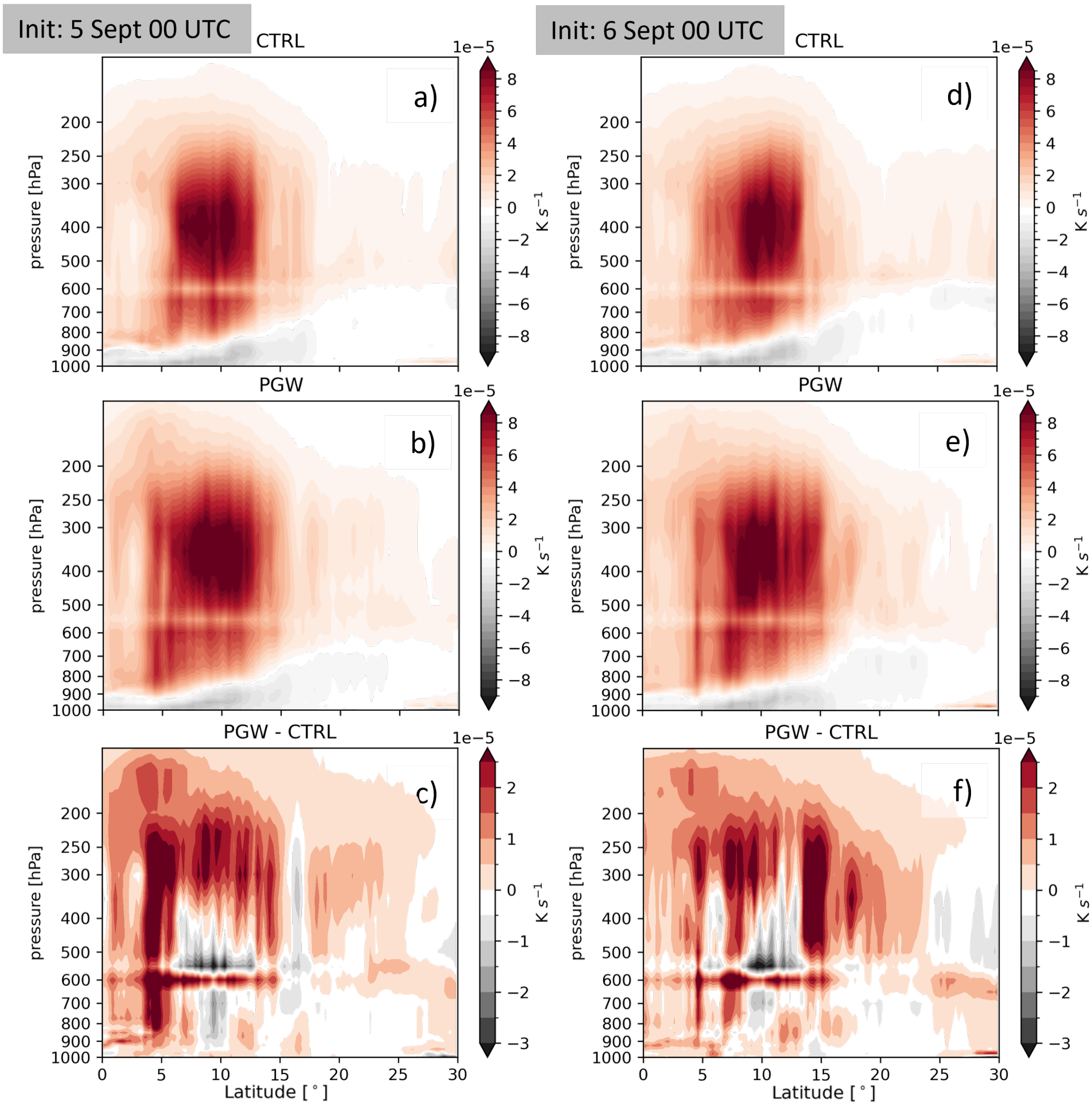

Figure S5. Vertical cross-section of the time-averaged diabatic heating rates from microphysics scheme removing the first 24 hours of the simulation for (a) CTRL, (b) PGW, and (c) the difference for 00 UTC, 5 September 2006 initialization. The same for (d), (e), and (f), respectively for 00 UTC, 6 September 2006 initialization. Longitude average taken for WAM box. Y axis is in log scale.

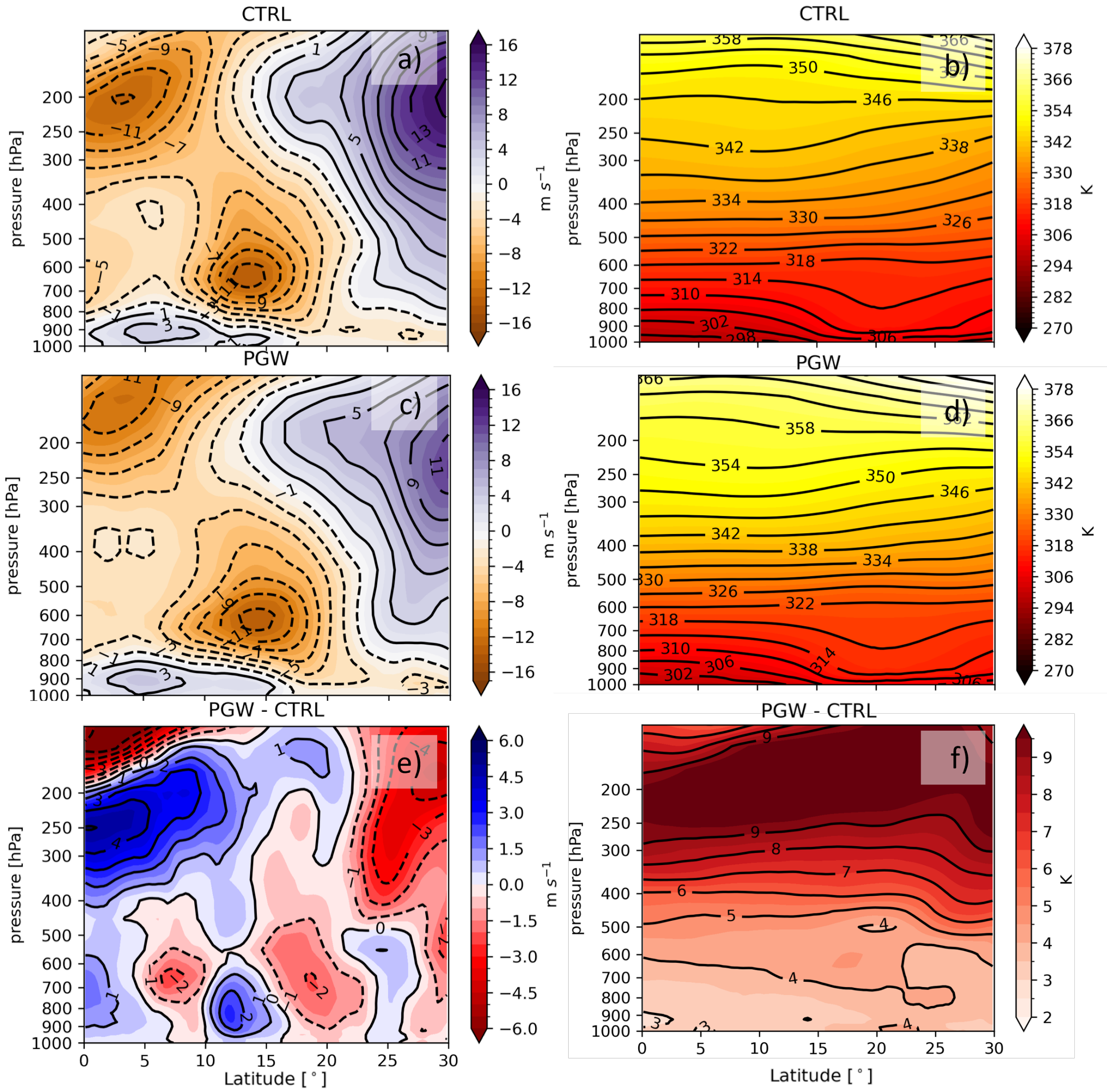

Figure S6. Vertical cross-section of the time-averaged zonal wind and potential temperature removing the first 24 hours of the simulation for CTRL in (a) and (b), respectively for 00 UTC, 5 September 2006 initialization. The same from (c-d) for PGW, and from (e-f) for the differences. Longitude average taken for the WAM box. Y axis is in log scale. The AEJ and TEJ are labeled in (a).

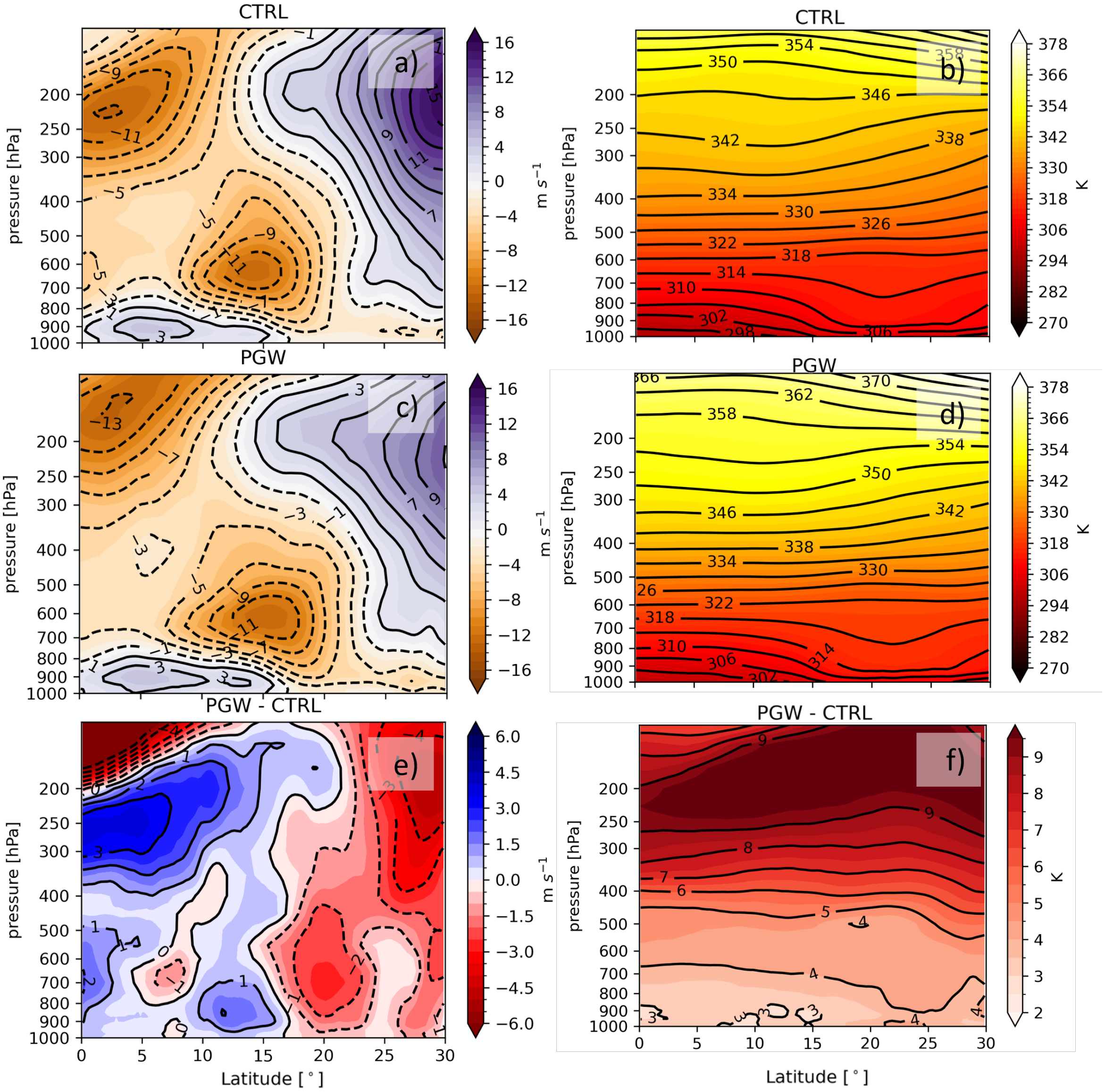

Figure S7. Vertical cross-section of the time-averaged zonal wind and potential temperature removing the first 24 hours of the simulation for CTRL in (a) and (b), respectively for 00 UTC, 6 September 2006 initialization. The same from (c-d) for PGW, and from (e-f) for the differences. Longitude average taken for the WAM box. Y axis is in log scale. The AEJ and TEJ are labeled in (a).